



Repositorio Institucional de la Universidad Autónoma de Madrid

<https://repositorio.uam.es>

Esta es la **versión de autor** del artículo publicado en:

This is an **author produced version** of a paper published in:

Journal of Medicinal Chemistry 58.13 (2016): 6265–6280

DOI: 10.1021/acs.jmedchem.6b00478

Copyright: © 2016, Elsevier Inc.

El acceso a la versión del editor puede requerir la suscripción del recurso

Access to the published version may require subscription

Gramine derivatives targeting Ca²⁺ channels and Ser/Thr phosphatases: a new dual strategy for the treatment of neurodegenerative diseases

Rocío Lajarán-Cuesta,[†] Carmen Nanclares,[†] Juan-Alberto Arranz-Tagarro,[†] Laura González-Lafuente,^{‡,||} Raquel L. Arribas,[†] Monique Araujo de Brito,[§] Luis Gandía,[†] Cristóbal de los Ríos^{,†,‡}*

[†]Instituto Teófilo Hernando and Departamento de Farmacología y Terapéutica, Facultad de Medicina, Universidad Autónoma de Madrid, C/ Arzobispo Morcillo, 4, 28029 Madrid, Spain

[§]Programa de Pós Graduação em Ciências Aplicadas a Produtos Para a Saúde, Faculdade de Farmácia, Universidade Federal Fluminense, Niterói, RJ, Brasil

[‡]Servicio de Farmacología Clínica, Instituto de Investigación Sanitaria, Hospital Universitario de la Princesa, C/ Diego de León, 62, 28006 Madrid, Spain

ABSTRACT

We describe the synthesis of gramine derivatives and their pharmacological evaluation as multipotent drugs for the treatment of Alzheimer's disease. An innovative multitarget approach is presented, targeting both voltage-gated Ca^{2+} channels, classically studied for neurodegenerative diseases, and Ser/Thr phosphatases, which have been marginally aimed, even despite their key role in protein τ dephosphorylation. Twenty five compounds were synthesized and mostly their neuroprotective profile exceeded that offered by the head compound gramine. In general, these compounds reduced the entry of Ca^{2+} through VGCC, as measured by Fluo-4/AM and patch clamp techniques, and protected in Ca^{2+} overload-induced models of neurotoxicity, like glutamate or veratridine exposures. Furthermore, we hypothesize that these compounds decrease τ hyperphosphorylation based on the maintenance of the Ser/Thr phosphatase activity and their neuroprotection against the damage caused by okadaic acid. Hence, we propose this multitarget approach as a new and promising strategy for the treatment of neurodegenerative diseases.

Introduction

Over a hundred years after Alois Alzheimer reported his observations describing a new neurodegenerative disease,¹ the battery of clinically approved drugs available to treat Alzheimer's disease (AD) patients is scarce and inefficient. Nowadays, AD patients are addressed with three cholinesterases (ChE) inhibitors (galantamine, donepezil, and rivastigmine), and memantine, a *N*-methyl-D-aspartate (NMDA) glutamate receptor blocker.² The former augments the levels of the neurotransmitter acetylcholine at the synapsis, under the rationale of the so-called "cholinergic hypothesis".³ Memantine avoids the altered Ca^{2+} uptake by neurons through the NMDA-sensitive ionic channel-coupled receptor, relying on the theory that all neurodegenerative diseases present an imbalanced Ca^{2+} homeostasis,³ so the reduction of the cytosolic Ca^{2+} concentration in neurons could slow down the progression of such diseases. Attempts to discover better drugs acting on any of these therapeutic targets have failed.⁴ Targeting the best-documented pathophysiological hallmarks of AD, that are senile plaques, mainly formed by the amyloid β peptide ($\text{A}\beta$),⁵ and neurofibrillary tangles (NFT) generated by the aggregation of the hyperphosphorylated microtubule-stabilizing τ protein,⁶ neither have supplied more successful therapies. To face amyloidogenesis, several strategies have been studied, e.g. compounds inhibiting the synthesis of $\text{A}\beta$ (α -secretase activators, both β - and γ -secretase inhibitors, among others) or its aggregation.⁷ As far as the τ -induced NFT formation, less work, but not negligible, has been carried out, mainly devoted to the preparation of kinase enzymes inhibitors, with the goal of hindering the hyperphosphorylation of τ , as the more phosphorylated τ protein is, the more susceptibility to its self-aggregation into NFT.⁸⁻⁹

Nevertheless, few of these approaches have supplied drugs eligible to be studied in clinical trials for AD. Many reasons could explain the lack of promising drugs for AD, but it seems quite likely that, as other neurodegenerative diseases, AD features a multifactorial origin, where various physiopathological events participate in the neuronal damage that leads to AD.¹⁰ Such hypothesis gave rise to the multi-target approach in drug discovery, which postulates that a drug, or the association of drugs, acting on two or more different biological targets that operate in the pathological process, could present a more beneficial effect on AD patients than a highly potent single-targeting drug.¹¹ Hence, during the last decade, a plethora of multi-target drug-based strategies have been described, by combining pharmacological interventions over ChE enzymes, A β peptides or the τ -induced NFT formation, among other therapeutic targets.¹²⁻¹⁵ In this regard, our research group has reported several families of multi-target drugs since 2000, with the control of neuronal Ca²⁺ homeostasis as the common target.¹⁶⁻¹⁹ Many evidences support the idea that pharmacological modulation of Ca²⁺ within neurons could mitigate the neurotoxicity present in a neurodegeneration scenario,²⁰ as that neurons having NFT present high activity of Ca²⁺-dependent protease enzymes,²¹ or that the presence of A β peptides elevates Ca²⁺ concentrations in resting neurons, sensitizing them for apoptosis phenomena.²²⁻²³ There is preclinical and clinical evidence that the blockade of voltage-gated Ca²⁺ channels (VGCC) may attenuate dementia, since an excessive and prolonged Ca²⁺ entry into the cytosol leads to neurodegeneration and neuronal loss.²⁴⁻²⁶ The VGCC blockade, both at presynaptic (P/Q- and N-type VGCC) and at postsynaptic sites (L-type VGCC), has shown a neuroprotective effect in different animal models of neurodegeneration and excitotoxicity, such as the blockade of ω -agatoxin IVA in a rat ischemia model (P/Q-VGCC blocker),²⁷ the blockade by the synthetic version of ω -conotoxin MVIIA in a traumatic diffuse brain injury model in rats (N-type VGCC blocker),²⁸ that of

verapamil in a focal ischemia model in rats (L-type VGCC blocker),²⁹ or those of nivaldipine and nitrendipine (L-type VGCC blockers) in an A β -induced toxicity model in mice.³⁰ Some VGCC antagonists have been tested in clinical trials for dementia and, according to the Cochrane report published in 2002, nimodipine can be of some efficacy for the treatment of AD.³¹

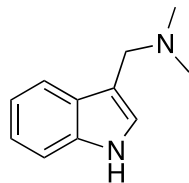
On the other hand, during the latest years, we have paid attention to the neurodegeneration elicited by the hyperphosphorylated τ protein and the subsequent intracellular NFT.³² The degree of τ phosphorylation depends on the enzymatic activity of both kinases and phosphatases.⁹

Tremendous scientific efforts have been invested in the development of kinase enzymes inhibitors, e.g. GSK3 β inhibitors,³³⁻³⁴ with scarce success. However, rather few contributions have aimed to promote the dephosphorylation process carried out by phosphatase enzymes,³⁵ mainly performed by the phosphoprotein phosphatases (PPP) 2A and 1 (PP2A and PP1, respectively).³⁶ PPP enzymes catalyze the hydrolysis of phosphate esters at Ser and Thr residues, being PP1 and PP2A responsible of the 90% of the cellular Ser/Thr phosphatase activity within healthy human brains.³⁶ In AD brains, total phosphatase activity is reduced by half, with PP2A, PP1, and PP5 activities decreased by 50%, 20%, and 20%, respectively.³⁶⁻³⁷ Regarding to PP2A, it is the most efficient τ phosphatase (accounts for over 70% of τ dephosphorylation).³⁵ The relationship between the AD-triggered neurodegeneration and the downregulation of PP2A activity has been widely demonstrated: in postmortem brains from AD patients, PP2A mRNA and protein levels are decreased,³⁸⁻³⁹ while the endogenous PP2A inhibitors I₁^{PP2A} (nuclear) and I₂^{PP2A} (cytoplasmatic) are increased by 20%;⁴⁰⁻⁴¹ it exists an augmented inactivation of the PP2A catalytic subunit (PP2Ac) through the phosphorylation at Y307 residue;⁴² the PP2A methylation rates at L309, responsible for the PP2A assembly to its regulatory subunits, is decreased;⁴³ there is also a reduced expression of B55 α , the main PP2A regulatory subunit mediating

dephosphorylation of τ , in frontal and temporal cortices.⁴⁴⁻⁴⁶ Moreover, PP2A dephosphorylates NMDA receptors at several NRx subunits, evoking a lesser Ca^{2+} influx through these receptors, what entails a neuroprotective effect against excitotoxicity, similarly to memantine.⁴⁷⁻⁴⁸ Although the leading role of PP2A is indisputable, other PPP enzymes, like PP1 and PP5, are also implicated in the pathology of AD.⁴⁹

Our research group described the neuroprotective properties of a multi-target drug that was able to inhibit cholinesterase enzymes and to maintain the PP2A-controlled phosphatase activity.⁵⁰ Confirming the correlation between NMDA and PP2A, ethyl 5-amino-2-methyl-6,7,8,9-tetrahydrobenzo[*b*][1,8]naphthyridine-3-carboxylate (ITH12246), protected rat hippocampal slices against the damage elicited by glutamate through a mechanism implicating PPP, as okadaic acid (OA), a selective inhibitor of PP1 and PP2A, reversed its neuroprotective signal. In addition, it reduced the loss of memory in mice subjected to scopolamine administration, as monitored by the object placement test.⁵¹

For all of these reasons, we considered worthwhile to keep deepening in the study of PPP enzymes as a part of a multi-target strategy to find new drugs for AD, remaining the control of cytosolic Ca^{2+} as the other main therapeutic target. In this work, we describe the findings observed with a family of indole derivatives, analogues to the natural alkaloid gramine (**1**, Figure 1), which has shown promising pharmacological activities.⁵²



1

Figure 1. Chemical structure of the alkaloid gramine (3-(dimethylaminomethyl)-1*H*-indole) (**1**).

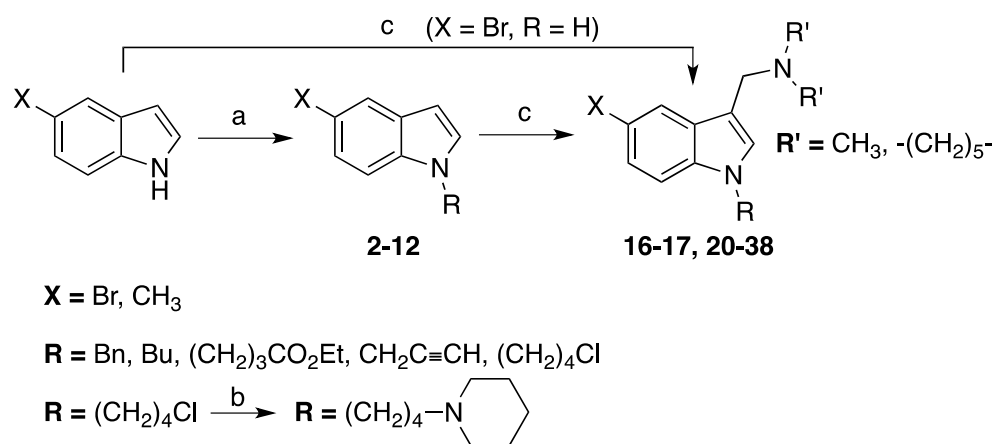
Indeed, some of its brominated derivatives have been described as Ca^{2+} channels blockers.⁵³ In our laboratory, we observed that **1** protected SH-SY5Y neuroblastoma cells against the toxic stimulus generated by OA in a wide range of concentrations. We wondered whether such huge neuroprotective effect was, at least in part, due to the activation of PPP enzymes. This prompted us to design a new family of **1** derivatives and evaluate their pharmacological activity as Ca^{2+} channel blockers and Ser/Thr phosphatase activators, as well as assessing their neuroprotective profile in several in vitro models of neurodegeneration. The results reported in this paper support the idea that scientific community devoted to the search of multi-target drugs must continue its efforts to offer original proposals for the discovery of new drugs for neurodegenerative diseases.

Results and Discussion

Chemistry. The design of **1** derivatives focused on favoring a potential Ca^{2+} channel blocking activity as well as the interaction with the principal dephosphorylating enzymes of τ , that are the Ser/Thr phosphatases. As two marine-derived bromo-substituted **1** analogs have been described to block VGCC,⁵³ we reasoned that our first family of synthesized **1** derivatives should possess a bromine atom at C5. Regarding to the binding to PP2A, previous studies of our research group detected a binding site close to the catalytic core in the PP2Ac subunit,⁵⁰ where specific ligands would not compromise the PP2A enzymatic activity, but alternatively would avoid the arrival of direct inhibitors to the catalytic machinery of PP2A. By preliminary computational studies, if

new indole-based ligands present a tiny hydrophobic substituent at C5, as well as a long hydrophobic moiety linked to the indole nitrogen, their affinity to this binding site would improve. Thus, a second family of **1** derivatives having a methyl group at C5 was designed, where the members of both families are differentially substituted at the indole nitrogen. The *N*-alkylation was carried out by nucleophilic substitution of alkyl halides in presence of NaH as a base (Scheme 1). Alkyl, benzyl or propargyl bromides and iodides suffered the nucleophilic attack of 5-substituted indoles in excellent yields, except for ethyl bromobutyrate, as only 5-bromoindole was able to lead to the formation of the ethyl indolylbutanoate **6** in low yields. Attempts to optimize this substitution, by using other bases such as KOH and solvents (DMF, CH₃CN, THF or acetone), phase-transfer catalysts, among other experimental conditions, were not satisfactory. The nucleophilic substitution over 1-chloro-4-iodobutane, leading to the *N*-(4'-chlorobutyl)-indoles **9** and **10**, allowed us to incorporate piperidine as a pending substituent, through a further nucleophilic attack of piperidine in acetonitrile, using K₂CO₃ as a base, obtaining the 5-bromo or 5-methyl-*N*-substituted derivatives **11** and **12**, respectively (Scheme 1). Polycations, such as polylysine and protamine, as well as highly basic compounds, specifically histones, were the first compounds found to activate PP2A in vitro.⁵⁴ This fact, together with other recently discovered positively charged modulators, e.g. memantine, led to establish basic cationic compounds as a family of PP2A activators.⁵⁵⁻⁵⁶ The head compound **1** possesses a basic amino group that is positively charged at physiological pH, so it could be classified as a cationic activator. In order to keep this property, all **1** derivatives conserve this basic amino group at C3, either as dimethylamine or piperidine group.

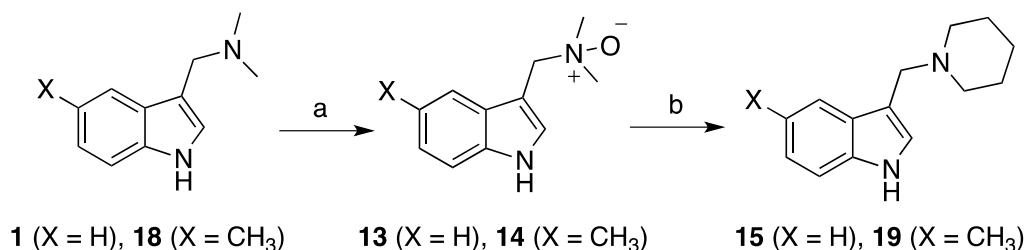
Scheme 1. Preparation of **1** derivatives"



“Reagents and Conditions: (a) (1) NaH, DMSO, rt, 1–2 h; (2) alkyl halide, rt, 1–12 h. (b) piperidine, MeCN, K₂CO₃, rt to 60 °C, 12 h. (c) Me₂NH or piperidine, HCHO (aq), AcOH, 0 °C to rt, 2 to 5 h.

The further Mannich type reaction furnished the desired C3-substituted **1** derivatives **20–38** in which the order of addition of reagents played an essential role, allowing us to reach excellent yields. 5-Bromoindole reacted with dimethylamine or piperidine at these conditions to form the *N*-unsubstituted **1** derivatives **16** and **17** in good yields (Scheme 1). However, the same protocol proposed for the reaction of 5-methylindole with piperidine, derived in a complex mixture of products. To sort this out, we selected an alternative method conducted through the generation of the *N*-oxide intermediate **14**, from the commercially available 5-methylgramine **18**, which is further treated with neat piperidine to form compound **19** in quantitative yield. The same strategy was proposed to prepare the piperidine-bearing analogue of **1**, that is compound **15**, synthesized and pharmacologically evaluated for comparative purposes (Scheme 2).

Scheme 2. Alternative route for the preparation of *N*-unsubstituted **1 derivatives^a**



“Reagents and conditions: (a) H₂O₂ (30% aq), EtOH, rt, 2 h. (b) piperidine, reflux, 3 h.

At this point, it is worthwhile mentioning that, despite the huge literature in both Organic and Medicinal Chemistry regarding to the syntheses and uses of 3-aminoethylindoles, backed by the Chemistry of the tryptophan, serotonin and melatonin, among other so-called biogenic amines,⁵⁷⁻⁵⁹ the study of the 3-aminomethylindoles analogs has been comparatively inappreciable. Indeed, **1** derivatives have been extensively used in Organic Synthesis as starting material for the preparation of serotonin-like natural products and potential drugs.⁶⁰⁻⁶¹ Among the reasons for this lack of interest, their delicate chemical stability in aqueous acid media seems to be the main reason.⁶² We confirmed by ¹H-NMR that 3-methylen-3*H*-indoles are formed as by-products after routine procedures such as silica gel-based flash chromatography purification or in the NMR analysis when using CDCl₃ as deuterated solvent. These pitfalls were avoided by executing the work-up at pH 14, neutralizing the organic solvents, mainly CH₂Cl₂, with basic alumina and, when necessary, purification with flash chromatography was carried out in basic alumina instead of silica gel, and NMR spectra were made in acetone-*d*₆. After confirming the structure and purity of final compounds **15–38**, with the aim of facilitating their manipulation and biological evaluation, they were salinized to hydrochloride or oxalate salts, by treatment with HCl in ether or oxalic acid in ethyl acetate solutions, respectively. Solvents for the salinization solutions were

previously dried over MgSO_4 to remove possible traces of water. We then confirmed structure and purity of the salinized compounds, and their chemical stability at physiological pH by monitoring ^{13}C and ^1H -NMR spectra in D_2O , not detecting any modification in the NMR signals after several days.

Pharmacological Evaluation. Effect of **1 derivatives 15–38 on the Ca^{2+} entry through**

VGCC. To evaluate the blocking activity of the new **1** derivatives, we stimulated SH-SY5Y neuroblastoma cells with an extracellular solution containing KCl 70 mM, leading to membrane depolarization and VGCC opening.⁶³ The SH-SY5Y neuroblastoma cell line is a reliable model to monitor cytosolic Ca^{2+} fluctuations in excitable cells, as it possesses VGCC and intracellular Ca^{2+} -buffering organelles similarly to regular primary neuronal cultures.⁶⁴⁻⁶⁵ Consequently, the SH-SY5Y cells, charged with the Ca^{2+} -sensitive fluorescent probe Fluo-4, suffered a rise in the cytosolic Ca^{2+} that was modulated by the presence of these potential VGCC blockers, tested at 1 μM (Table 1). Eleven out 24 compounds reduced the high K^+ -evoked cytosolic Ca^{2+} increase in a statistically significant manner. Considering the data expressed in Table 1, some structure-activity relationships can be inferred. Most of the compounds that block VGCC bear a piperidinylmethyl substituent at C3; compound **20** ($\text{X} = \text{Br}$, $\text{R} = \text{Bn}$) was the only dimethylaminomethyl-substituted compound, together with **1**, that reduced the Ca^{2+} increase. As far as the *N*-alkylation, the benzyl moiety affords the best blockade of Ca^{2+} increase, but also butyl, chlorobutyl, and propargyl groups are optimal substituents, whose results are fairly better when compounds present additionally a bromine atom at C5 and a piperidine at C3, instead of methyl and dimethylamine, respectively. It is already known in literature that bromo-substitution at the indole core provides compounds with Ca^{2+} antagonist activity.⁵³ The blocking effect of compounds that present a bulky substituent at the indole nitrogen (**27**, **28**, **35–38**) substantially

dropped to below 20%. The well-known VGCC blocker nifedipine,⁶⁶ used as a standard at 3 μM , reduced Ca^{2+} increase by 73% in these experiments. With the goal of deepening into their Ca^{2+} -antagonist effect, we carried out electrophysiological techniques, performing patch-clamp experiments in the whole-cell configuration. We studied the effect on Ca^{2+} (I_{Ca}) currents of **1**, the best VGCC blockers of the family (**21**, **25**, **30**, and **33**), and three more compounds (**20**, **23**, and **26**) that showed important neuroprotective and/or pro-phosphatases properties (see below). Current vs. voltage (I/V) curves, from -60 to $+60$ mV as depolarizing potentials, were initially performed in absence of compounds, to select the depolarizing pulse that featured the highest I_{Ca} . Then, bovine chromaffin cells were subjected to 50 ms depolarizing pulses every 20 s at the potential at which maximal I_{Ca} was obtained, usually 0 mV; after reaching a stable response, cells were perfused with the different compounds until a maximal blockade degree was achieved. Figure S1 of supporting info reflects a typical register of I_{Ca} , dealing with a control situation. Under these experimental conditions, compounds **1**, **21**, **23**, **25**, and **26** blocked I_{Ca} in a statistically significant manner (Figure 2), confirming their VGCC blocking properties.

Table 1. Blockade by compounds 15–38 of the Ca^{2+} entry elicited by K^+ 70 mM-evoked depolarization in SH-SY5Y cells, measured by the Ca^{2+} -sensitive probe Fluo-4/AM^a

Comp.	X	R	R'	% Blockade
Nifedipine ^b	-	-	-	$73 \pm 5^{***}$
1	H	H	CH_3	$25 \pm 7^{**}$
15	H	H	$-(\text{CH}_2)_5-$	$30 \pm 4^{**}$
16	Br	H	CH_3	$3 \pm 3^{\text{ns}}$

17	Br	H	-(CH ₂) ₅ -	7 ± 7 ^{ns}
18	CH ₃	H	CH ₃	10 ± 5 ^{ns}
19	CH ₃	H	-(CH ₂) ₅ -	16 ± 6 ^{ns}
20	Br	Bn	CH ₃	38 ± 6 ^{***}
21	Br	Bn	-(CH ₂) ₅ -	45 ± 3 ^{***}
22	CH ₃	Bn	CH ₃	18 ± 6 ^{ns}
23	CH ₃	Bn	-(CH ₂) ₅ -	22 ± 9 [*]
24	Br	<i>n</i> -Bu	CH ₃	14 ± 6 ^{ns}
25	Br	<i>n</i> -Bu	-(CH ₂) ₅ -	63 ± 4 ^{***}
26	CH ₃	<i>n</i> -Bu	-(CH ₂) ₅ -	21 ± 6 [*]
27	Br	-(CH ₂) ₃ CO ₂ Et	CH ₃	13 ± 6 ^{ns}
28	Br	-(CH ₂) ₃ CO ₂ Et	-(CH ₂) ₅ -	16 ± 3 ^{ns}
29	Br	CH ₂ C≡CH	CH ₃	10 ± 5 ^{ns}
30	Br	CH ₂ C≡CH	-(CH ₂) ₅ -	42 ± 3 ^{***}
31	CH ₃	CH ₂ C≡CH	CH ₃	14 ± 6 ^{ns}
32	CH ₃	CH ₂ C≡CH	-(CH ₂) ₅ -	25 ± 7 ^{**}
33	Br	-(CH ₂) ₄ Cl	-(CH ₂) ₅ -	57 ± 6 ^{***}
34	CH ₃	-(CH ₂) ₄ Cl	-(CH ₂) ₅ -	35 ± 5 ^{***}
35	Br	-(CH ₂) ₄ Pi	CH ₃	14 ± 6 ^{ns}
36	Br	-(CH ₂) ₄ Pi	-(CH ₂) ₅ -	19 ± 7 [*]
37	CH ₃	-(CH ₂) ₄ Pi	CH ₃	16 ± 7 ^{ns}
38	CH ₃	-(CH ₂) ₄ Pi	-(CH ₂) ₅ -	4 ± 3 ^{ns}

^aData are mean of at least six experiments ± SEM comparing with the K⁺-induced Ca²⁺ increase in absence of compounds. Compounds assayed at 1 μM. ****p* < 0.001, ***p* < 0.01, **p* < 0.05, and ns = not significant. ^b Tested at 3 μM. Pi = piperidinyl.

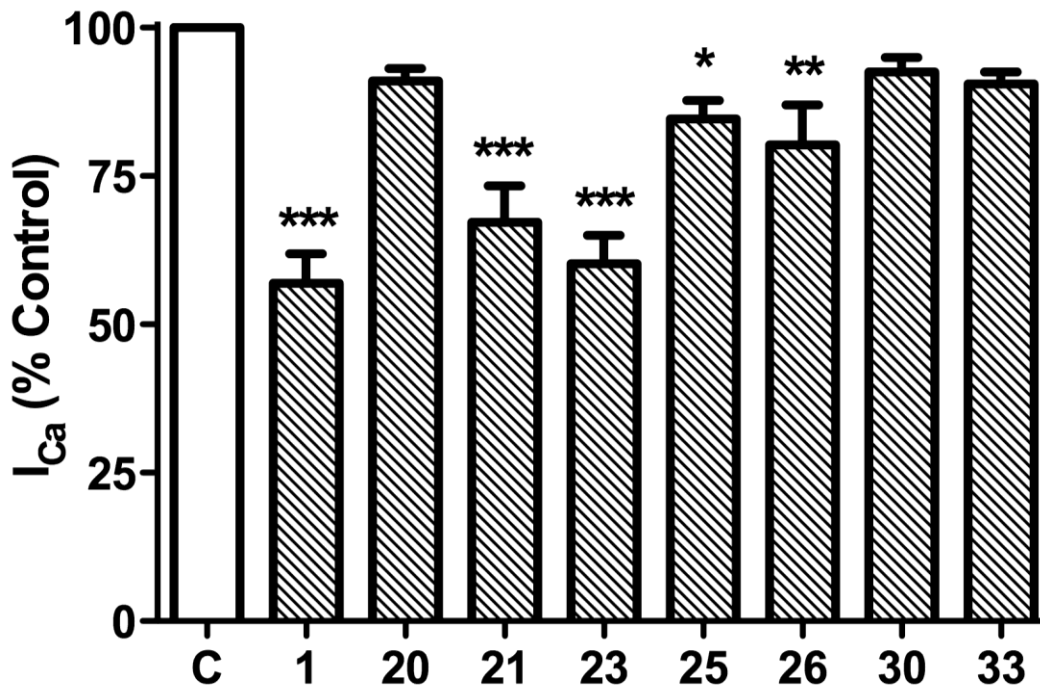


Figure 2. Depolarization-evoked Ca^{2+} currents (I_{Ca}) in bovine chromaffin cells. Whole-cell I_{Ca} were recorded using 2 mM Ca^{2+} as charge carrier and -80 mV as holding potential. Averaged results, of at least 7 cells of independent batches, representing normalized remaining I_{Ca} in presence of selected **1** derivatives at the concentration of 1 μ M. *** $p < 0.001$, ** $p < 0.01$, * $p < 0.05$, comparing with control in absence of compounds (C, white bar).

Of note is the differential behavior of these compounds between the two experimental procedures realized, i.e. the fluorescent-based assay and the patch-clamp techniques. This could be interpreted in base of the different expression of VGCC subtypes between SH-SY5Y cells, where 50% of them are L-subtype,⁶⁴ and bovine chromaffin cells, which only present a 20% of the L-subtype.⁶⁷ Such hypothesis raised an important point, as compound **23** blocked I_{Ca} in bovine chromaffin cells by 40% (Figure 2), but it only reduced the fluorescence-monitored Ca^{2+} increase in SH-SY5Y by 22% (Table 1), so we wondered whether compound **23** could be

selectively blocking the non L-subtypes of VGCC, what it would be of interest taking into account the lack of efficient pharmacological tools available to selectively interact to such non-L VGCC,⁶⁸ either N- or P/Q subtypes. For this reason, we further registered the VGCC blocking effect of compound **23** in presence of the selective L-type VGCC blocker nifedipine, as well as in presence of the N and P/Q type VGCC blocker ω -conotoxin MVIIC,⁶⁹ as shown in Figure 3. Compound **23** exerted an additional blockade of the I_{Ca} in the presence of nifedipine (Figure 3A and 3C), but on the contrary, the I_{Ca} observed in the presence of ω -conotoxin MVIIC remained constant when compound **23** was administered (Figure 3B and 3C). Therefore, we can conclude that compound **23** is a selective non-L VGCC blocker.

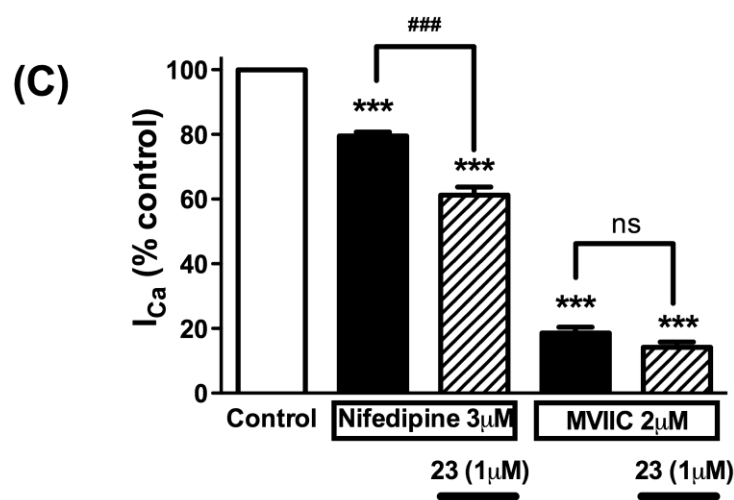
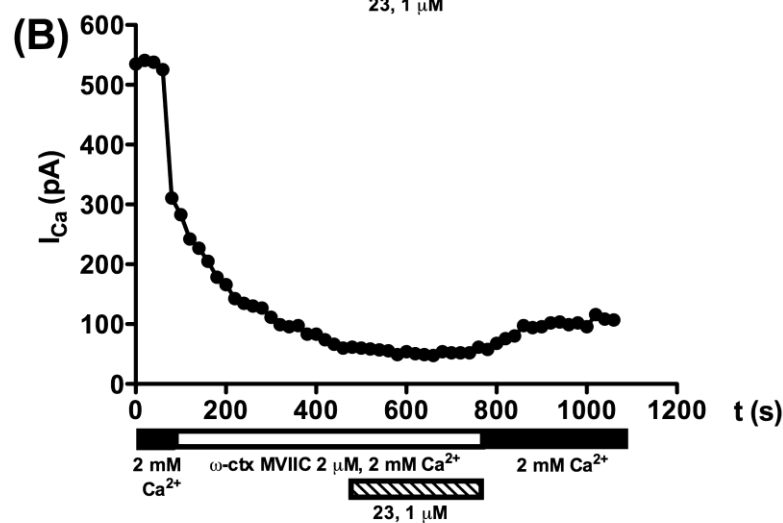
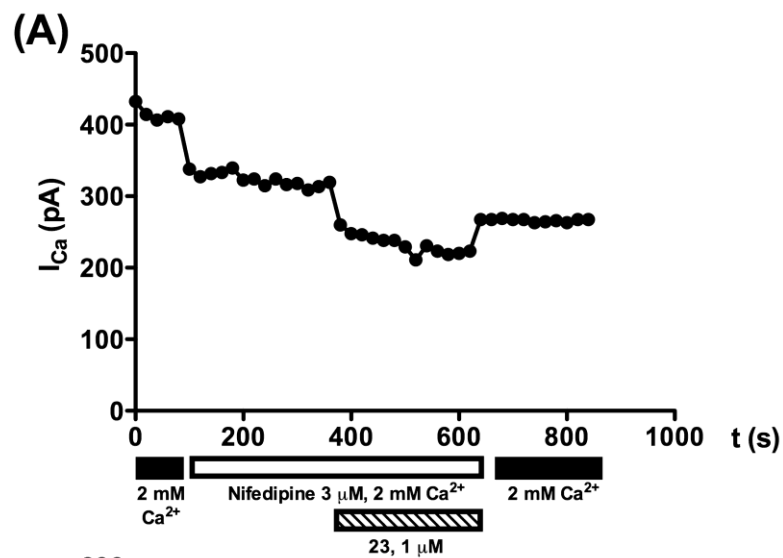


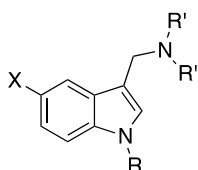
Figure 3. Compound **23** partially blocks non-L type Ca^{2+} currents. Bovine chromaffin cells, voltage-clamped at -80 mV, were challenged with 50 ms depolarizing pulses to 0 mV at 20 s intervals. Ca^{2+} 2 mM was used as charge carrier. Panel A shows typical Ca^{2+} currents (I_{Ca}) time course in a cell perfused with nifedipine 3 μM (L-type VGCC blocker) alone and in the presence of compound **23** at 1 μM . Panel B shows a typical I_{Ca} time course in a cell perfused with ω -conotoxin (ω -ctx) MVIIC 2 μM (N- and P/Q-type Ca^{2+} VGCC blocker) alone and in the presence of compound **23** at 1 μM . Panel C shows the averaged peak amplitude of I_{Ca} with respect to control (white bar) in the presence of either nifedipine or MVIIC alone (black columns) or concomitantly with compound **23** (stripped columns). Data are means \pm SEM of 16 cells for each treatment from 3 different cell cultures. *** $p < 0.001$, respect to cells depolarized in absence of drugs (control group), ### $p < 0.001$, ns = not significant.

Effect of 1 derivatives 15–38 on the Ser/Thr phosphatase activity. As mentioned in the introduction, the Ser/Thr phosphatase activity of PP1 and PP2A is impaired in neurodegeneration scenarios,³⁶ leading to the augmentation of the phosphorylation rate in τ protein, and thus favoring its self-aggregation to form the NFT. This reduction in the phosphatase activity is mainly ascribed to the concurrence of endogenous inhibitors that bind at the catalytic site of PPP, hindering the hydrolysis of phosphate esters at Ser or Thr amino acids.⁴⁰ The use of the PP1 and PP2 inhibitor OA is a reliable model of these pathological processes, as it has been described that it tightly binds catalytic subunits of both enzymes.⁷⁰ Indeed, the administration of OA to rodents mimicked the morphological hallmarks of AD.⁷¹ Hence, to appraise the effect of compounds **15–38** on the activity of PPP enzymes, we subjected SH-SY5Y cells to the exposure of OA at 15 nM, an adequate concentration to inhibit both PP1 and PP2A,⁷²⁻⁷³ in the presence of the testing

compounds, estimating the resulting phosphatase activity by the colorimetric method of the *p*-nitrophenylphosphate (pNPP). The pNPP is a colorless substance that turns yellow (absorbance 405 nm) when is hydrolyzed to *p*-nitrophenol by the action of phosphatase enzymes.⁷⁴ Under these experimental conditions, OA diminished the total phosphatase activity by a 32%, and 12 out of 25 compounds reduced the deprival of total phosphatase activity in a statistically significant manner, being the best compounds able to maintain such enzymatic activity a 40% higher than with OA in absence of compounds (Table 2). Although OA interacts exclusively with the Ser/Thr phosphatases PP1 and PP2A, due to the Tyr phosphatase activity is much more extended in nervous system than the Ser/Thr phosphatase activity, we decided to study the effect of the compounds in presence of the Tyr phosphatase inhibitor sodium orthovanadate,⁷⁵ administered to the SH-SY5Y cells at 1 mM, so the phosphatase activity recorded by the pNPP probe would be only derived from Ser/Thr phosphatase enzymes. Pretty much similar data were found; half of the compounds counteracted the OA-induced reduction of the Ser/Thr phosphatase activity in a statistically significant manner (Table 2). Regarding to structure-activity relationships, either no substitution at the indole nitrogen (R = H), benzyl group or a butyl group, seem to be the most optimal alternatives as R substituents, as hit compound **1** offers a satisfactory pro-phosphatase activity, similarly to compounds **15**, **16**, **18**, **20**, **23**, **24**, **25**, and **31**.

Collectively, compounds **15**, **23**, and **25**, together with the hit compound **1**, featured a multitarget activity, as they demonstrated both pro-phosphatase and Ca²⁺ channels blocking activities, in all the experimental protocols implemented. In parallel, we evaluated the capability of the **1** derivatives **15–38** to protect against neuronal damage in in vitro models of neurodegeneration resembling AD.

Table 2. Effect of 1 derivatives 15–38 on the Ser/Thr phosphatase activity depressed by okadaic acid (OA)^a



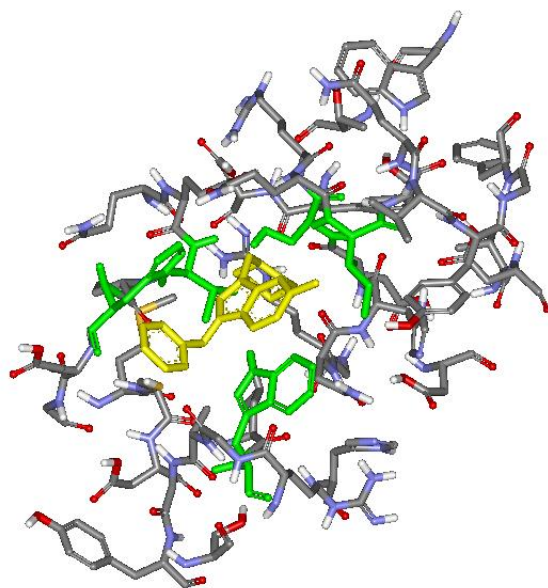
Comp.	X	R	R'	%Total phosphatase activity	%Ser/Thr phosphatase activity
Control	-	-	-	100	100
OA	-	-	-	68 ± 2 ^{###}	61 ± 3 ^{###}
Memantine	-	-	-	77 ± 3 [*]	78 ± 5 ^{***}
1	H	H	CH ₃	80 ± 5 [*]	76 ± 5 [*]
15	H	H	-(CH ₂) ₅ -	76 ± 4 [*]	79 ± 8 [*]
16	Br	H	CH ₃	80 ± 4 ^{**}	76 ± 6 [*]
17	Br	H	-(CH ₂) ₅ -	74 ± 4 ^{ns}	67 ± 3 ^{ns}
18	CH ₃	H	CH ₃	79 ± 4 [*]	77 ± 4 [*]
19	CH ₃	H	-(CH ₂) ₅ -	71 ± 3 ^{ns}	69 ± 5 ^{ns}
20	Br	Bn	CH ₃	81 ± 4 ^{**}	78 ± 5 [*]
21	Br	Bn	-(CH ₂) ₅ -	79 ± 4 [*]	70 ± 7 ^{ns}
22	CH ₃	Bn	CH ₃	73 ± 3 ^{ns}	66 ± 5 ^{ns}
23	CH ₃	Bn	-(CH ₂) ₅ -	77 ± 4 [*]	78 ± 6 [*]
24	Br	<i>n</i> -Bu	CH ₃	81 ± 6 [*]	76 ± 4 [*]
25	Br	<i>n</i> -Bu	-(CH ₂) ₅ -	78 ± 3 [*]	79 ± 4 ^{**}
26	CH ₃	<i>n</i> -Bu	-(CH ₂) ₅ -	69 ± 2 ^{ns}	66 ± 6 ^{ns}
27	Br	(CH ₂) ₃ CO ₂ Et	CH ₃	76 ± 7 ^{ns}	66 ± 4 ^{ns}
28	Br	(CH ₂) ₃ CO ₂ Et	-(CH ₂) ₅ -	73 ± 2 ^{ns}	71 ± 3 [*]
29	Br	CH ₂ C≡CH	CH ₃	70 ± 5 ^{ns}	64 ± 4 ^{ns}
30	Br	CH ₂ C≡CH	-(CH ₂) ₅ -	77 ± 3 ^{**}	72 ± 5 ^{ns}
31	CH ₃	CH ₂ C≡CH	CH ₃	80 ± 4 [*]	74 ± 9 [*]
32	CH ₃	CH ₂ C≡CH	-(CH ₂) ₅ -	71 ± 3 ^{ns}	66 ± 7 ^{ns}
33	Br	-(CH ₂) ₄ Cl	-(CH ₂) ₅ -	68 ± 3 ^{ns}	62 ± 7 ^{ns}
34	CH ₃	-(CH ₂) ₄ Cl	-(CH ₂) ₅ -	71 ± 4 ^{ns}	62 ± 6 ^{ns}
35	Br	-(CH ₂) ₄ Pi	CH ₃	73 ± 5 ^{ns}	68 ± 5 ^{ns}

36	Br	-(CH ₂) ₄ Pi	-(CH ₂) ₅ -	73 ± 2 [*]	70 ± 4 ^{ns}
37	CH ₃	-(CH ₂) ₄ Pi	CH ₃	74 ± 3 ^{ns}	68 ± 5 ^{ns}
38	CH ₃	-(CH ₂) ₄ Pi	-(CH ₂) ₅ -	72 ± 3 ^{ns}	70 ± 5 [*]

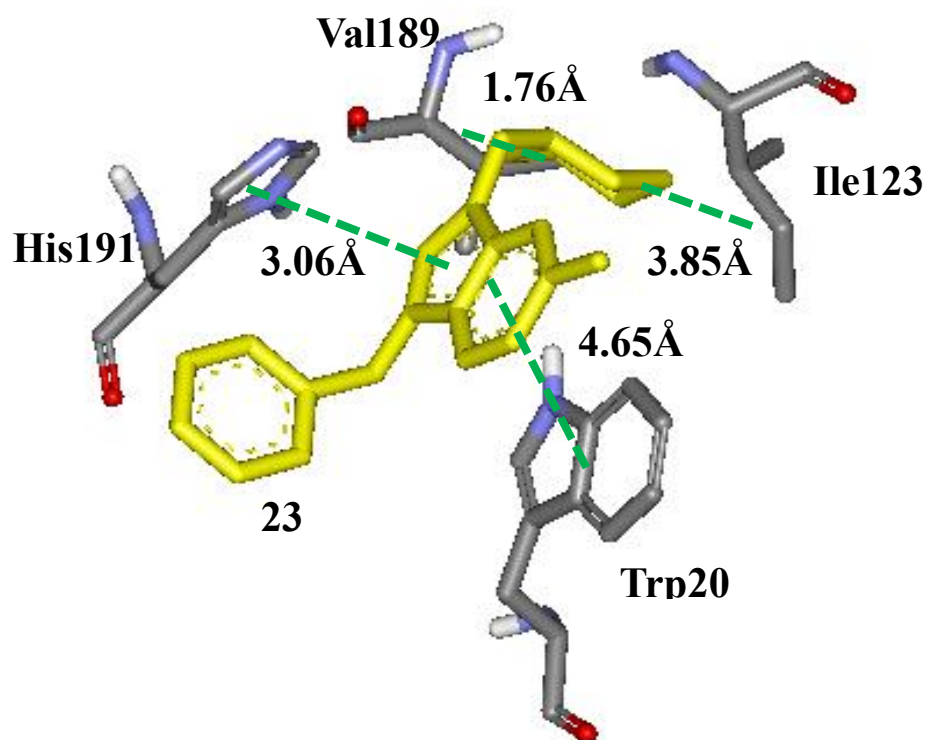
^aSH-SY5Y cells were treated with compounds at 0.1 μM in presence of the PPP inhibitor okadaic acid (OA) at 15 nM. Data are mean of at least four experiments ± SEM, expressed as percentage respect to control situation, where cells were not treated with compounds neither OA. ^{###}*p* < 0.001, respect to control; ^{***}*p* < 0.001, ^{**}*p* < 0.01, ^{*}*p* < 0.05, and ns = not significant, respect to cells only treated with OA. Phosphatase activity was evaluated by the method of the pNPP. To estimate Ser/Thr phosphatase activity, the Tyr phosphatase inhibitor sodium orthovanadate at 1 mM was applied to the experiments. Pi = piperidinyl.

Docking studies. We selected compound **23** to exemplify the interaction between the main τ protein phosphatase, i.e. PP2A, with these **1** derivatives, because of its significant phosphatase activity (Table 2), as well as its neuroprotective activity counteracting the damage provoked by OA and Glu (Table 3 and Figure 5, see below). The complex of PP2A and compound **23** revealed van der Waals interactions between the piperidine ring of compound **23** and the side chain of residues Ile123 (d = 3.85 Å) and Val189 (d = 1.76 Å) (Figure 4B). The indole ring of compound **23** also interacts with both the imidazole ring of His191 (d = 3.06 Å) and the indole ring of the Trp200 (d = 4.65 Å), probably in a hydrophobic π- π stacking contact (Figure 4B). OA also interacted with Ile123, His191 and Trp200, as previously reported by Xing *et al.*, 2006.⁷⁰ Also, the nitrogen of the piperidine ring of compound **23** probably makes a strong hydrogen bond with the hydroxyl group of Ser120 (d = 1.66 Å) (Figure 4C), which contributes to the affinity of the ligand in this binding site of PP2A (Figure 4A).

(A)



(B)



(C)

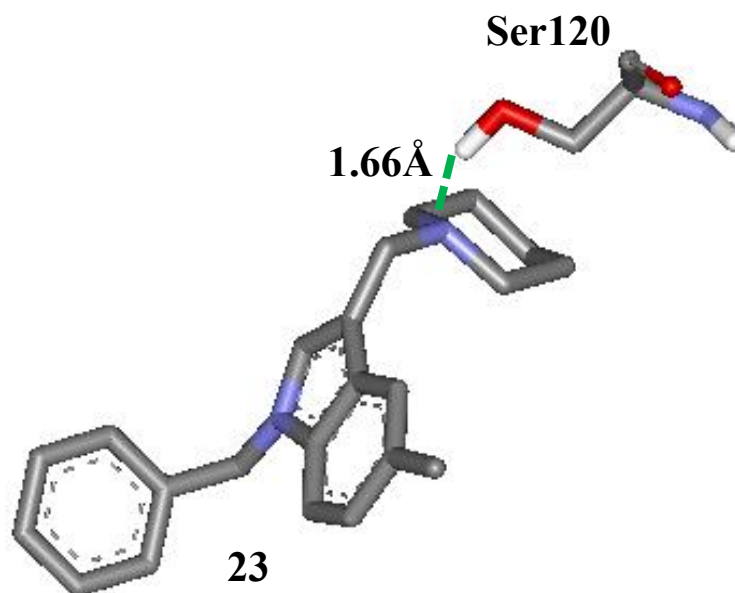


Figure 4. Docking of the compound **23**–PP2A complex. (A) Pose of compound **23** (yellow) in the PP2Ac binding site (main residues in green). (B) Van der Waals contacts (Val189 and Ile123) and hydrophobic π interactions (His191 and Trp200) of compound **23** (yellow). (C) Hydrogen bond between compound **23** and Ser120.

Neuroprotection experiments. Since we had found some bioactive compounds, the raised question was whether these **1** derivatives, by regulating the neuronal Ca^{2+} homeostasis and the Ser/Thr phosphatase activity, would be able to protect neurons against neurotoxic stimuli related to AD. We monitored cell viability with the method of the 3-(4,5-dimethylthiazol-2-yl)-2,5-diphenyltetrazolium bromide (MTT) reduction,⁷⁶ in in vitro neuronal models subjected to Ca^{2+} overload or τ hyperpolarization. Since VGCC and Ser/Thr phosphatases, targeted by our **1**

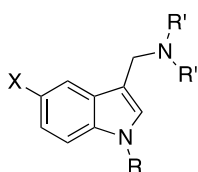
derivatives, present highlighted physiological roles, we firstly assessed the potential per se toxicity of compounds **15–38** in the neuronal models object of study, i.e. cortical motor neurons and SH-SY5Y neuroblastoma cells. As graphed in Figures S2 and S3 of supporting info, none of the compounds, incubated for 48 h, reduced the cell viability of SH-SY5Y cells at concentrations lower than 10 μ M. In the case of cortical motor neurons, compounds **15** and **36** marginally reduced cell viability when incubated for 48 h at 1 μ M (Figures S4 and S5, supporting info).

In order to emulate a Ca^{2+} overload, cortical motor neurons were exposed to veratridine 20 μ M, a voltage-gated Na^+ channels (VGNC) ligand that delays their inactivation, leading to a depolarization-elicited Ca^{2+} entry.⁷⁷ After 24 h pre-incubation of the compounds, at 1 μ M, neurons were co-incubated for another 24 h with veratridine, inducing a loss of viability of about 50% (Table 3). More than a half of the compounds, but not **1**, reduced the veratridine-induced damage in a significant manner. Compounds **23**, **25**, and **26** stood out by rescuing the neuronal viability by a 50% or more. In these experiments, the presence of piperidine at C3 instead of dimethylamine seems to favor this neuroprotective activity. Again, benzyl and butyl groups branched to the indole nitrogen afforded the best neuroprotection (Table 3). The VGNC blocker tetrodotoxin (TTX) was used as standard in these experiments.⁷⁸

In parallel, we tested the neuroprotective activity of compounds **15–38** against a model of τ hyperphosphorylation, by stimulating SH-SY5Y neuroblastoma cells with the PPP selective inhibitor OA. SH-SY5Y cells suffered a fall of 35% in their viability when exposed for 20 h to OA 20 nM. Under this situation, most of compounds noticeably mitigated the reduction in the cell viability caused by OA, and 10 of them did it by 50% or more, being the best compound **25** (Table 3). Melatonin was used as standard in these experiments.⁷⁹ Among all the structure-

activity relationships considered, we appreciated outstanding activities when the compounds present benzyl, butyl or no substitution at the indole nitrogen.

Table 3. %Neuroprotection of 1 derivatives 15–38 on the cell viability of cortical motor neurons and SH-SY5Y neuroblastoma cells damaged with veratridine and okadaic acid, respectively^a



Comp.	X	R	R'	Veratridine ^b	Okadaic acid ^c
TTX	-	-	-	77 ± 1 ^{***}	-
Melatonin	-	-	-	-	43 ± 3 ^{***}
1	H	H	CH ₃	0 ± 4 ^{ns}	45 ± 2 ^{***}
15	H	H	-(CH ₂) ₅ -	18 ± 7 ^{ns}	47 ± 5 ^{**}
16	Br	H	CH ₃	11 ± 5 ^{ns}	47 ± 4 ^{**}
17	Br	H	-(CH ₂) ₅ -	19 ± 3 [*]	60 ± 5 ^{**}
18	CH ₃	H	CH ₃	30 ± 5 [*]	59 ± 4 ^{**}
19	CH ₃	H	-(CH ₂) ₅ -	7 ± 3 ^{ns}	38 ± 3 ^{***}
20	Br	Bn	CH ₃	34 ± 3 ^{***}	56 ± 3 ^{***}
21	Br	Bn	-(CH ₂) ₅ -	36 ± 6 ^{**}	54 ± 6 ^{**}
22	CH ₃	Bn	CH ₃	35 ± 9 [*]	44 ± 4 [*]
23	CH ₃	Bn	-(CH ₂) ₅ -	51 ± 6 ^{**}	56 ± 5 ^{**}
24	Br	<i>n</i> -Bu	CH ₃	34 ± 5 ^{**}	66 ± 5 ^{**}
25	Br	<i>n</i> -Bu	-(CH ₂) ₅ -	72 ± 7 ^{***}	71 ± 3 ^{***}
26	CH ₃	<i>n</i> -Bu	-(CH ₂) ₅ -	60 ± 7 ^{***}	46 ± 5 [*]
27	Br	(CH ₂) ₃ CO ₂ Et	CH ₃	42 ± 6 [*]	58 ± 2 ^{**}
28	Br	(CH ₂) ₃ CO ₂ Et	-(CH ₂) ₅ -	36 ± 7 [*]	43 ± 5 [*]
29	Br	CH ₂ C≡CH	CH ₃	17 ± 5 ^{ns}	12 ± 4 ^{ns}
30	Br	CH ₂ C≡CH	-(CH ₂) ₅ -	24 ± 4 [*]	47 ± 3 ^{**}
31	CH ₃	CH ₂ C≡CH	CH ₃	14 ± 10 ^{ns}	12 ± 3 ^{ns}

32	CH ₃	CH ₂ C≡CH	-(CH ₂) ₅ -	19 ± 5 ^{ns}	42 ± 8 ^{ns}
33	Br	-(CH ₂) ₄ Cl	-(CH ₂) ₅ -	39 ± 6 [*]	48 ± 8 [*]
34	CH ₃	-(CH ₂) ₄ Cl	-(CH ₂) ₅ -	36 ± 5 ^{**}	56 ± 6 [*]
35	Br	-(CH ₂) ₄ Pi	CH ₃	21 ± 9 ^{ns}	31 ± 3 ^{**}
36	Br	-(CH ₂) ₄ Pi	-(CH ₂) ₅ -	0 ± 5 ^{ns}	61 ± 4 ^{***}
37	CH ₃	-(CH ₂) ₄ Pi	CH ₃	4 ± 6 ^{ns}	37 ± 1 ^{***}
38	CH ₃	-(CH ₂) ₄ Pi	-(CH ₂) ₅ -	1 ± 5 ^{ns}	26 ± 3 ^{**}

^aCell viability was measured by the method of the MTT reduction. Data are expressed as the percentage of cell viability recovered in cells treated with the toxic stimulus plus compounds, comparing with viability of cells only exposed to veratridine or OA; mean of at least 5 experiments ± SEM in triplicate. ****p* < 0.001, ***p* < 0.01, **p* < 0.05, and ns = not significant, respect to cells only treated with veratridine or OA. ^bCortical motor neurons exposed to veratridine 20 μM in presence of compounds at 1 μM, except for compound **36** which was tested at 0.1 μM due to its toxicity at 1 μM (see Figure S5 supporting info). ^cSH-SY5Y neuroblastoma cells exposed to OA 20 nM in presence of compounds at 0.1 μM. Pi = piperidinyl.

Gathering all the pharmacological data obtained, we proposed that these new **1** derivatives are multitarget neuroprotective compounds able to interact with two pathophysiological events affected in AD, i.e. Ca²⁺ dishomeostasis and Ser/Thr phosphatases inhibition, and in turn entailing a neuroprotective profile, according to the in vitro models of neurodegeneration we have performed. Overall, it can be extrapolated that the presence of benzyl or butyl groups at the indole nitrogen along with a piperidine at C3, preferentially offer privileged structures of **1** derivatives, according to the pharmacological activities object of study, and their consequent neuroprotective properties over AD-resembling neurodegeneration models. However, neuroprotective compounds historically fail in their pharmacological actions when they are evaluated in more physiological models of experimental study. Therefore, we carry out a more

physiological model of biological evaluation, defined by the use of rat hippocampal slices subjected to toxic stimuli related to AD, recording the ability of selected compounds to counteract the tissue damage.^{17, 50, 63, 80} In this preparation, neurons are surrounded by their natural environment, e.g. glia cells, extracellular matrix, etc. Rat hippocampi were subjected to a sustained exposition to the excitatory neurotransmitter glutamate, which is considered a close model to the excitotoxicity occurred in neurodegeneration.⁸¹ In addition, recent contributions have hypothesized that PP2A can down-regulate the Ca^{2+} influx through the NMDA receptors, as dephosphorylation of NR1A subunit by this phosphatase accelerates the desensitization rate of the NMDA receptor.^{48, 82-83} Hence, this model has proven to be an excellent experimental protocol to test the neuroprotective activities of either Ca^{2+} -antagonists or Ser/Thr phosphatase activators. Tested compounds were selected according to optimal biological activities and neuroprotective properties in vitro, as well as chemical diversity (Figure 5).

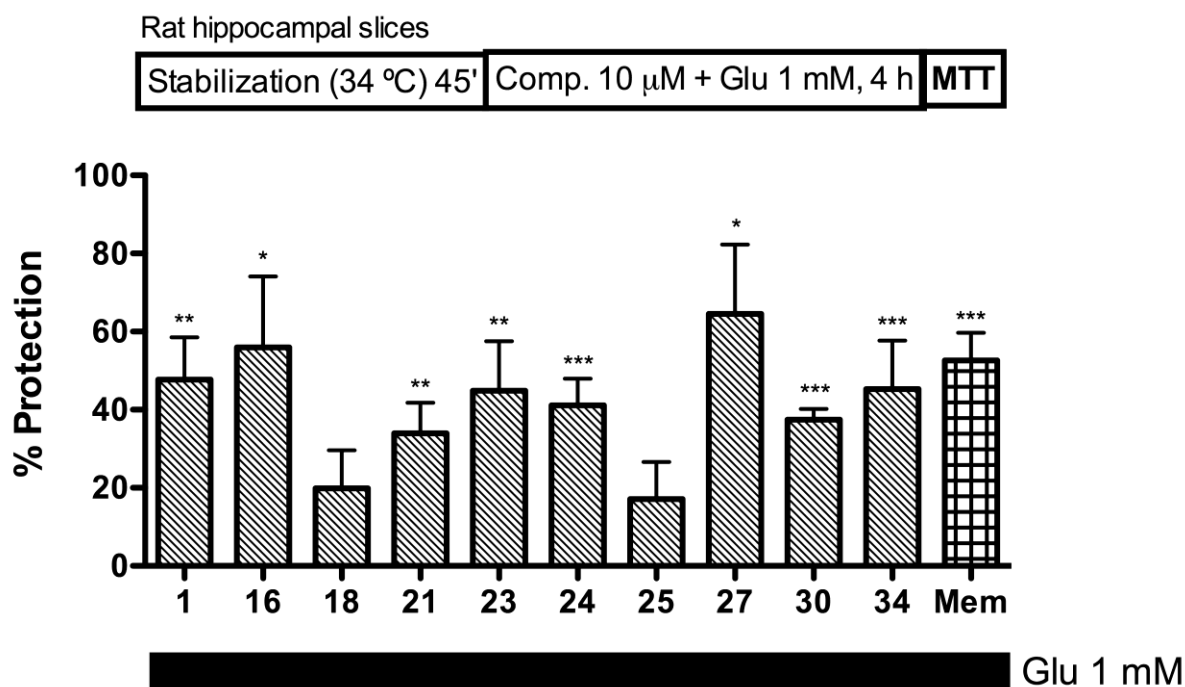


Figure 5. Effect of selected **1** derivatives on the viability of rat hippocampal slices damaged with glutamate (Glu) 1 mM, measured through the MTT reduction. %Protection respect to the viability of hippocampal slices treated with Glu in absence of compounds. Data are expressed as mean \pm SEM of at least 4 different tissue batches in quadruplicate. $###p < 0.001$ respect to basal. $***p < 0.001$, $**p < 0.01$, $*p < 0.05$, respect to slices only treated with Glu.

Compounds **21**, **23**, and **30** that had evinced regulating activities of both Ca^{2+} entry and Ser/Thr phosphatases, and protected neurons in both veratridine and OA-based models of neurodegeneration, avoided the glutamate-induced loss of viability of the hippocampal slices by 30% or more, however the multitarget and in vitro neuroprotectant compound **25** failed to protect such preparations. Compounds **16**, **18**, and **24**, behaved as Ser/Thr phosphatase activators (Table 2), and had a proper in vitro neuroprotection profile. Nevertheless, in this model, only

compounds **16** and **24** reasserted that neuroprotective properties, as they reduced the damage by glutamate by 40% or more (Figure 5). Compound **34** also protected hippocampi from the glutamate excitotoxicity, according to its in vitro neuroprotection properties (Table 3), although it had only targeted the cell Ca^{2+} signal (Table 1). Compound **27** protected against both Ca^{2+} overload and τ hyperphosphorylation, but it did not show any activity on either depolarization-evoked Ca^{2+} entry or Ser/Thr phosphatase. In addition, it substantially protected hippocampal slices against the glutamate exposure (Figure 5); one possibility is that compound **27** would be affecting other pathways involved in the neuronal death/survival scenarios.

Conclusions

This work illustrates an alternative approach for a multitarget strategy for the treatment of AD, by devising a double interaction with neuronal Ca^{2+} signal and Ser/Thr phosphatase activity. Regulation of cytosolic Ca^{2+} concentrations by different VGCC blockers has been a pharmacology target widely studied for several neurodegenerative diseases, but few contributions has selected it as a part of a multitarget-based drug development, which have mostly inclined towards the complement of cholinesterases inhibition with $\text{A}\beta$ down-regulation or τ hyperphosphorylation reduction strategies, affording unfruitful results. Regarding to the τ hyperphosphorylation, the research works have almost exclusively focused on the development of protein τ kinase inhibitors. We propose that the activation, or the reduction of inhibitory actions, over protein τ phosphatase enzymes, deserves more attention, overcoming the historical prejudice of their unspecificity, currently rebutted.³² Of note is that, when we recorded the phosphatase activity by the method of the pNPP (Table 2), a substantial decrease of 70% was

computed in cells exposed to the Tyr phosphatase inhibitor VO_3^- , what confirms that Tyr phosphatase activity is much more extended than Ser/Thr phosphatase activity in nervous system. The fact that τ protein is mainly dephosphorylated by PP1 and PP2A entails the advantage that Ser/Thr phosphatase activators would not present such sizeable off-target pharmacology as Tyr phosphatase activators **would**. To finish up, we hypothesize that compound **23** is an eligible lead compound to further investigate its pharmacological activities in preclinical models of AD, as it demonstrated significant activity over VCGG and Ser/Thr phosphatases, accompanied by a wide-spectrum neuroprotective profile. The fact that compound **23** exerts Ca^{2+} blockade preferentially through non-L type VGCC is in agreement to the rising interest of developing both N- and P/Q type VGCC blockers for dementia,^{68, 84} what supposes a breakthrough in the study of Ca^{2+} antagonists for central nervous system diseases because they could bypass the cardiovascular side effects resulting from peripheral L-type channel blockade,²⁵⁻
²⁶ Hence, the **1** derivative 1-benzyl-5-methyl-3-(piperidin-1-ylmethyl)-1*H*-indole (compound **23**, which we have named ITH12657) features an innovative multitarget-based mechanism of action, aiming neuronal Ca^{2+} control and Ser/Thr phosphatase activity.

Experimental Section

General Procedures. 5-**B**romoindole, 5-methylindole, **1**, compound **18**, and general reagents were purchased from Sigma-Aldrich (Madrid, Spain). Solvents were purchased from VWR (Barcelona, Spain). Reactions were monitored by thin layer chromatography aluminum oxide on TLC-PET foils (Sigma-Aldrich). Detection was made with UV light at 254 nm. All the reactions were subjected to Schlenk conditions (vacuum purges and argon atmosphere). Pre-charged basic

aluminum oxide (Brockmann I) columns were used in a Biotage chromatographic station. Melting points were determined in a Stuart apparatus (SMP-10) and are not corrected. MS spectra were obtained in a QSTAR de ABSciex apparatus. ^1H and ^{13}C NMR spectra were carried out with a Bruker AVANCE 300 MHz and described as ppm using deuterated solvents as internal standard. All the compounds described and pharmacologically tested had a purity of 95% or more determined by elemental analysis performed on a LECO CHNS-932 station (C, H, and N within 0.4% of the calculated values for the proposed formula). None of the tested compounds present structural similarities with Pan Assay Interference Compounds (PAINS), according to the classification reported by Baell and Holloway.⁸⁵

General Method for the Synthesis of *N*-alkyl-5-bromo(or methyl)indoles 2–10. The method described by Na et al.⁸⁶ was followed, with slight modifications. Briefly, to a solution of 5-bromo-1*H*-indole or 5-methyl-1*H*-indole (1 equiv) in anhydrous dimethyl sulfoxide (DMSO) (1.4–5 mL/mmol), NaH (1.2 equiv, 60%, dispersed in mineral oil) was added under inert gas at room temperature. After the reaction mixture was stirred for 1–2 h, the corresponding alkyl halide (1.2–1.7 equiv) was added and stirred for 1–2 h more (with exception of the synthesis of **6**, which required overnight), monitored by TLC. When the reaction was completed, it was stopped by addition of water (10 mL/mmol) and extracted with neutralized CH_2Cl_2 (3 × 30 mL/mmol). The organic layer was dried over anhydrous Na_2SO_4 , filtered and evaporated, to obtain a yellow oil that did not require purification, except for compound **6**.

1-Benzyl-5-bromo-1*H*-indole (2). Following the general method for the synthesis of *N*-alkyl-5-bromo(or methyl)indoles **2–10**, reaction of 5-bromo-1*H*-indole (500 mg, 2.55 mmol) in anhydrous DMSO (13 mL) with NaH (122 mg, 3.06 mmol) and benzyl bromide (363 μL , 3.06 mmol) yielded **2** (740 mg, >99%) with spectral data according to literature.⁸⁷

1-Benzyl-5-methyl-1*H*-indole (3). Following the general method for the synthesis of *N*-alkyl-5-bromo(or methyl)indoles **2–10**, reaction of 5-methyl-1*H*-indole (150 mg, 1.14 mmol) in anhydrous DMSO (5.71 mL) with NaH (55 mg, 1.37 mmol) and benzyl bromide (163 μ L, 1.37 mmol) yielded **3** (282 mg, >99%) with spectral data according to literature.⁸⁸

5-Bromo-1-butyl-1*H*-indole (4). Following the general method for the synthesis of *N*-alkyl-5-bromo(or methyl)indoles **2–10**, reaction of 5-bromo-1*H*-indole (200 mg, 1.02 mmol) in anhydrous DMSO (5 mL) with NaH (48 mg, 1.22 mmol) and 1-iodobutane (139 μ L, 1.22 mmol) yielded **4** (242 mg, 94%). ¹H NMR (300 MHz, CDCl₃) δ 7.75 (d, 1H, *J* = 1.8 Hz, H4), 7.27 (dd, 1H, *J* = 1.9, 8.7 Hz, H6), 7.19 (d, 1H, *J* = 8.7 Hz, H7), 7.09 (d, 1H, *J* = 3.1 Hz, H2), 6.42 (d, 1H, *J* = 3.1 Hz, H3), 4.09 (t, 2H, *J* = 7.1 Hz, NCH₂), 1.81 (m, 2H, NCH₂CH₂), 1.36–1.24 (m, 2H, CH₂CH₃), 0.94 (t, 3H, *J* = 7.3 Hz, CH₃).

1-Butyl-5-methyl-1*H*-indole (5). Following the general method for the synthesis of *N*-alkyl-5-bromo(or methyl)indoles **2–10**, reaction of 5-methyl-1*H*-indole (200 mg, 1.52 mmol) in anhydrous DMSO (7.62 mL) with NaH (73 mg, 1.83 mmol) and 1-iodobutane (208 μ L, 1.83 mmol) yielded **5** (235 mg, 82%). ¹H NMR (300 MHz, acetone-*d*₆): δ 7.38 (m, 1H, H4), 7.29 (d, 1H, *J* = 8.4 Hz, H7), 7.16 (d, 1H, *J* = 3.1 Hz, H2), 7.01 (dd, 1H, *J* = 1.6, 8.4 Hz, H6), 6.37 (dd, 1H, *J* = 0.8, 3.1 Hz, H3) 4.11 (t, 2H, = 7.0 Hz, NCH₂), 2.44 (s, 3H, CH₃), 1.78 (m, 2H, NCH₂CH₂), 1.35–1.24 (m, 2H, CH₂CH₃), 0.93 (t, 3H, *J* = 7.4 Hz, CH₂CH₃).

Ethyl 4-(5-bromo-1*H*-indol-1-yl)butanoate (6). Following the general method for the synthesis of *N*-alkyl-5-bromo(or methyl)indoles **2–10**, reaction of 5-bromo-1*H*-indole (500 mg, 2.55 mmol) in anhydrous DMSO (10 mL) with NaH (122 mg, 3.06 mmol) and ethyl 4-bromobutanoate (461 μ L, 3.06 mmol) obtaining a yellow solid that was purified by automatized

flash chromatography with ethyl acetate/hexane mixtures as eluent, yielding **6** (281 mg, 36%). ¹H NMR (300 MHz, acetone-*d*₆) δ 7.76 (d, 1H, *J* = 1.8 Hz, H4), 7.42 (d, 1H, *J* = 8.7 Hz, H7), 7.31–7.26 (m, 2H, H2, H6), 6.47 (dd, 1H, *J* = 0.6, 3.1 Hz, H3), 4.24 (t, 2H, *J* = 7.0 Hz, NCH₂), 4.09 (c, 2H, *J* = 7.1 Hz, OCH₂), 2.28 (t, 2H, *J* = 6.8 Hz, CH₂CO), 2.10 (m, 2H, NCH₂CH₂), 1.20 (t, 3H, *J* = 7.1 Hz, CH₃).

5-Bromo-1-(prop-2-yn-1-yl)-1*H*-indole (7). Following the general method for the synthesis of *N*-alkyl-5-bromo(or methyl)indoles **2–10**, reaction of 5-bromo-1*H*-indole (200 mg, 1.02 mmol) in anhydrous DMSO (2.5 mL) with NaH (48 mg, 1.22 mmol) and 3-bromoprop-1-yne (136 μL, 1.22 mmol) yielded **7** (235 mg, >99%), with spectral data according to literature.⁸⁹

5-Methyl-1-(prop-2-yn-1-yl)-1*H*-indole (8). Following the general method for the synthesis of *N*-alkyl-5-bromo(or methyl)indoles **2–10**, reaction of 5-methyl-1*H*-indole (150 mg, 1.14 mmol) in anhydrous DMSO (2.29 mL) with NaH (55 mg, 1.37 mmol) and 3-bromoprop-1-yne (153 μL, 1.372 mmol) yielded **8** (190 mg, >99%). ¹H NMR (300 MHz, acetone-*d*₆) δ 7.51 (m, 1H, H4), 7.41 (d, 1H, *J* = 8.3 Hz, H7), 7.28 (d, 1H, *J* = 3.2 Hz, H2), 7.16 (dd, 1H, *J* = 1.5, 8.4 Hz, H6), 6.54 (dd, 1H, *J* = 0.8, 3.2 Hz, H3), 4.88 (d, 2H, *J* = 2.6 Hz, CH₂), 2.91 (t, 1H, *J* = 2.6 Hz, CH), 2.39 (s, 3H, CH₃).

5-Bromo-1-(4-chlorobutyl)-1*H*-indole (9). Following the general method for the synthesis of *N*-alkyl-5-bromo(or methyl)indoles **2–10**, reaction of 5-bromo-1*H*-indole (1 g, 5.10 mmol) in anhydrous DMSO (7 mL) with NaH (245 mg, 6.12 mmol) and 1-chloro-4-iodobutane (1.1 mL, 8.67 mmol) yielded **9** (1.4 g, >99%). ¹H NMR (300 MHz, CDCl₃) δ 7.77 (d, 1H, *J* = 1.8 Hz, H4), 7.30 (dd, 1H, *J* = 1.9, 8.7 Hz, H6), 7.20 (d, 1H, *J* = 8.7 Hz, H7), 7.09 (d, 1H, *J* = 3.1 Hz, H2),

6.45 (dd, 1H, $J = 0.6, 3.1$ Hz, H3), 4.13 (t, 2H, $J = 6.9$ Hz, NCH₂), 3.50 (t, 2H, $J = 6.4$ Hz, CH₂Cl), 2.05–1.93 and 1.80–1.68 (2m, 4H, ClCH₂CH₂CH₂).

1-(4-Chlorobutyl)-5-methyl-1H-indole (10). Following the general method for the synthesis of *N*-alkyl-5-bromo(or methyl)indoles **2–10**, reaction of 5-methyl-1H-indole (200 mg, 1.52 mmol) in anhydrous DMSO (6 mL) with NaH (73 mg, 1.83 mmol) and 1-chloro-4-iodobutane (317 μ L, 2.59 mmol) yielded **10** (340 mg, >99%). ¹H NMR (300 MHz, acetone-*d*₆) δ 7.38 (m, 1H, H4), 7.31 (d, 1H, $J = 8.4$ Hz, H7), 7.18 (d, 1H, $J = 3.1$ Hz, H2), 7.01 (dd, 1H, $J = 1.3$ Hz, $J = 8.4$ Hz, H6), 6.38 (dd, 1H, $J = 0.7, 3.1$ Hz, H3), 4.15 (t, 2H, $J = 6.9$ Hz, NCH₂), 3.53 (t, 2H, $J = 6.6$ Hz, CH₂Cl), 2.43 (s, 3H, CH₃), 1.98–1.87 and 1.76–1.65 (2m, 4H, ClCH₂CH₂CH₂).

General Method for the synthesis of 4-(piperidin-1-yl)butyl)indoles 11 and 12. The method of Martelli et al.⁹⁰ was followed with slight modifications. To a solution of 1-(4-chlorobutyl)indole **9** or **10** (1 equiv) and piperidine (1.2 equiv) in CH₃CN (6.9 mL/mmol), anhydrous K₂CO₃ (1–2 equiv) was added at room temperature. The reaction mixture was stirred at 60 °C overnight, under inert gas. When the reaction did not further evolve, monitored by TLC, it was cooled down and neutralized CH₂Cl₂ (10 mL/mmol) was added. The mixture was then basified with NaOH 10%_{aq} (30 mL/mmol), extracted with neutralized CH₂Cl₂ (2 \times 30 mL/mmol), dried over anhydrous Na₂SO₄, filtered, and evaporated under vacuum. The crude was purified by automatized flash chromatography in basic alumina with ethyl acetate/hexane mixtures as eluent, obtaining a colorless oil.

5-Bromo-1-(4-(piperidin-1-yl)butyl)-1H-indole (11). Following the general method for the synthesis of 4-(piperidin-1-yl)butyl)indoles **11** and **12**, reaction of **9** (107 mg, 0.37 mmol) with piperidine (44 μ L, 0.45 mmol) and anhydrous K₂CO₃ (52 mg, 0.37 mmol) yielded **11** (70 mg,

60%). ^1H NMR (300 MHz, acetone- d_6) δ 7.72 (d, 1H, J = 1.8 Hz, H4), 7.44 (d, 1H, J = 8.7 Hz, H7), 7.33 (d, 1H, J = 3.1 Hz, H2), 7.24 (dd, 1H, J = 1.9, 8.7 Hz, H6), 6.43 (dd, 1H, J = 0.7, 3.2 Hz, H3), 4.22 [t, 2H, J = 7.1 Hz, $\text{NCH}_2(\text{CH}_2)_3\text{N}$], 2.33–2.19 [m, 6H, $\text{N}(\text{CH}_2)_3\text{CH}_2\text{N}$, H2'], 1.85 [m, 2H, $\text{NCH}_2\text{CH}_2(\text{CH}_2)_2\text{N}$], 1.54–1.29 [m, 8H, $\text{N}(\text{CH}_2)_2\text{CH}_2\text{CH}_2\text{N}$, H3', H4'].

5-Methyl-1-(4-(piperidin-1-yl)butyl)-1H-indole (12). Following the general method for the synthesis of 4-(piperidin-1-yl)butyl)indoles **11** and **12**, reaction of **10** (328 mg, 1.48 mmol) with piperidine (176 μL , 1.78 mmol) and anhydrous K_2CO_3 (409 mg, 2.96 mmol), yielded **12** (180 mg, 45%). ^1H NMR (300 MHz, acetone- d_6) δ 7.36 (m, 1H, H4), 7.32 (d, 1H, J = 8.4 Hz, H7), 7.17 (d, 1H, J = 3.1 Hz, H2), 6.98 (dd, 1H, J = 1.2, 8.1 Hz, H6), 6.35 (dd, 1H, J = 0.7, 3.1 Hz, H3), 4.13 [t, 2H, J = 7.1 Hz, $\text{NCH}_2(\text{CH}_2)_3\text{N}$], 2.42 (s, 3H, CH_3), 2.32–2.19 [m, 6H, $\text{N}(\text{CH}_2)_3\text{CH}_2\text{N}$, H2'], 1.83 [m, 2H, $\text{NCH}_2\text{CH}_2(\text{CH}_2)_2\text{N}$], 1.57–1.28 [m, 8H, $\text{N}(\text{CH}_2)_2\text{CH}_2\text{CH}_2\text{N}$, H3', H4'].

General Method for the synthesis of 15 and 19 through N-oxide intermediates. Based on the method of Henry and Leete,⁹¹ with modifications. To a suspension of **1** or *N,N*-dimethyl-1-(5-methyl-1H-indol-3-yl)methanamine (1 equiv) in absolute ethanol (0.4 mL/mmol), H_2O_2 (30 %; 0.3 mL/mmol) was added, under inert gas at room temperature, observing a slight exothermicity and the complete dissolution of the suspension. Then, the magnet stir was removed and the flask cooled down with an ice bath and thus kept overnight. The white crystals formed were washed with absolute ethanol and the supernatant was discarded. After confirming the formation of the corresponding *N*-oxide by ^1H NMR, they were dissolved in piperidine (4 mL/mmol) and refluxed for 3 hours. Piperidine was evaporated under vacuum and the crude recrystallized in absolute ethanol to obtain pure compounds.

3-(Piperidin-1-ylmethyl)-1*H*-indole (15). Following the general method for the synthesis of **15** and **19** through *N*-oxide intermediates, reaction of **1** (200 mg, 1.15 mmol) with H₂O₂ (30 %; 0.3 mL) in absolute ethanol (0.46 mL), yielded the 1-(1*H*-indol-3-yl)-*N,N*-dimethylmethanamine oxide **13**⁹¹ that was immediately used with no further purification. ¹H NMR (300 MHz, CD₃OD) δ 7.70 (ddd, 1H, *J* = 0.8, 1.4, 7.7 Hz, H4), 7.56 (s, 1H, H2), 7.42 (ddd, 1H, *J* = 0.8, 1.2, 8.0 Hz, H7), 7.21–7.10 (m, 2H, H5, H6), 4.61 (s, 2H, CH₂), 3.11 [s, 6H, (CH₃)₂]. Reaction of **13** (230 mg, 1.21 mmol) in piperidine (4.6 mL) yielded **15** (191 mg, 74%) as a brown crystal. Mp 142–144 °C. ¹H NMR (300 MHz, CD₃OD) δ 7.64 (d, 1H, *J* = 7.8 Hz, H4), 7.39 (m, 1H, H7), 7.24 (s, 1H, H2), 7.16–7.02 (m, 2H, H5, H6), 3.76 (s, 2H, CH₂), 2.56 (m, 4H, H2'), 1.63 (m, 4H, H3'), 1.52–1.41 (m, 2H, H4'). ¹³C NMR (75.4 MHz, CD₃OD) δ 137.8, 129.6, 126.3, 122.3, 120.0, 119.6, 112.2, 110.7, 55.0, 54.3, 26.4, 25.1. Anal. Calcd for C₁₄H₁₈N₂: C, 78.46; H, 8.47; N, 13.07. Found: C, 78.05; H, 8.39; N, 13.09

5-Methyl-3-(piperidin-1-ylmethyl)-1*H*-indole (19). Following the general method for the synthesis of **15** and **19** through *N*-oxide intermediates, reaction of *N,N*-dimethyl-1-(5-methyl-1*H*-indol-3-yl)methanamine (**18**) (40 mg, 0.21 mmol) with H₂O₂ (30 %; 60 μL) in absolute ethanol (85 μL), yielded *N,N*-dimethyl-1-(5-methyl-1*H*-indol-3-yl)methanamine oxide **14** that was immediately used with no further purification. Reaction of **14** (32 mg, 0.16 mmol) in piperidine (640 μL) yielded **19** (36 mg, >99%). ¹H NMR (300 MHz, CD₃OD) δ 7.40 (m, 1H, H4), 7.24 (d, 1H, *J* = 8.3 Hz, H7), 7.17 (s, 1H, H2), 6.95 (dd, 1H, *J* = 1.3, 8.3 Hz, H6), 3.72 (s, 2H, CH₂), 2.54 (m, 4H, H2'), 2.43 (s, 3H, CH₃), 1.60 (m, 4H, H3'), 1.51–1.38 (m, 2H, H4'). Its oxalate salt was prepared by dropwise addition of a solution of oxalic acid 1M (1 equiv) in ethyl acetate, under inert gas, to the compound previously dissolved in ethyl acetate dried over MgSO₄. After 2 h stirring, the salt was isolated by centrifugation, the mother liquid decanted, and the traces of

solvent removed under vacuum. Mp 186–188 °C. ^{13}C NMR (75.4 MHz, DMSO- d_6) δ 163.9, 134.3, 128.6, 128.1, 127.7, 123.2, 117.9, 111.6, 102.1, 51.1, 50.6, 22.4, 21.3, 21.2. Anal. Calcd for $\text{C}_{15}\text{H}_{20}\text{N}_2 \cdot \text{H}_2\text{O} \cdot \text{C}_2\text{H}_2\text{O}_4$: C, 60.70; H, 7.19; N, 8.33. Found: C, 60.73; H, 6.89; N, 8.29

General Method for the synthesis of 1 derivatives 16–18 and 20–38. The method of Miranda et al.⁹² was followed with modifications. Under argon atmosphere, dimethylamine (40%_{aq}) or piperidine (1–1.5 equiv) and formaldehyde (37%_{aq}, 1–2 equiv) were stirred in glacial acetic acid (0.3–5.5 mL/mmol) for 10 min to form the iminium ion, which was then added to a solution of 5-bromo-1*H*-indole or compounds **2–12** (1 equiv) in glacial acetic acid (0.1–2 mL/mmol) at 0 °C. After 5 min, reaction was allowed to reach room temperature and was stirred for 2–5 h, until the reaction was terminated or no evolution was observed by TLC. Then, NaOH_{aq} (30%) was added to get a pH 14. The mixture was extracted with neutralized CH_2Cl_2 (3 \times 30 mL/mmol) and the organic layer dried over anhydrous Na_2SO_4 , filtered and evaporated.

Oily compounds were salinized to hydrochloride or oxalate salts. Hydrochloride salts were prepared by dropwise addition of a solution of hydrochloric acid 1M in diethyl ether (1 equiv), under inert gas, to the compounds previously dissolved in ether (10 mL). Oxalate salts were prepared by dropwise addition of a solution of oxalic acid 1M in ethyl acetate (1 equiv), under inert gas, to the compound previously dissolved in ethyl acetate (10 mL). Both types of salts were kept under stirring for 2h, isolated by centrifugation and the traces of solvent removed under vacuum. Solvents for the salinization solutions were previously dried over MgSO_4 .

1-(5-Bromo-1*H*-indol-3-yl)-*N,N*-dimethylmethanamine (16) Following the general method for the synthesis of **1** derivatives **16–18** and **20–38**, reaction of 5-bromo-1*H*-indole (200 mg, 1.02

mmol) with dimethylamine (129 μ L, 1.02 mmol) and formaldehyde (76 μ L, 1.02 mmol) in glacial acetic acid (1 mL) yielded **16** as a brown solid that did not required further purification (234 mg, 80%). Mp 134–137 °C. ^1H NMR (300 MHz, CDCl_3) δ 8.35 (bs, 1H, NH), 7.84 (d, 1H, J = 1.6 Hz, H4), 7.32–7.23 (dd, 1H, J = 1.8, 8.4 Hz, H6), 7.20 (d, 1H, J = 8.6 Hz, H7), 7.10 (s, 1H, H2), 3.58 (s, 2H, CH_2), 2.28 [s, 6H, $\text{N}(\text{CH}_3)_2$]. ^{13}C NMR (75.4 MHz, acetone- d_6) δ 136.6, 130.7, 126.5, 124.8, 123.0, 114.0, 113.8, 112.5, 55.7, 45.5 [$\text{N}(\text{CH}_3)_2$]. Anal. Calcd for $\text{C}_{11}\text{H}_{13}\text{BrN}_2$: C, 52.19; H, 5.18; N, 11.07. Found: C, 51.89; H, 5.12; N, 10.64.

5-Bromo-3-(piperidin-1-ylmethyl)-1H-indole (17). Following the general method for the synthesis of **1** derivatives **16–18** and **20–38**, reaction of 5-bromo-1H-indole (200 mg, 1.02 mmol) with piperidine (99 μ L, 1.02 mmol) and formaldehyde (76 μ L, 1.02 mmol) in glacial acetic acid (0.5 mL) yielded **17** as a yellow solid that did not required further purification (238 mg, 80%). Mp 131–134 °C. ^1H NMR (300 MHz, acetone- d_6) δ 10.28 (bs, 1H, NH), 7.89 (d, 1H, J = 2.0 Hz, H4), 7.34 (dd, 1H, J = 0.3, 8.6 Hz, H7), 7.25 (d, 1H, J = 2.3 Hz, H2), 7.20 (dd, 1H, J = 2.0, 8.6 Hz, H6), 3.59 (d, 2H, J = 0.7 Hz, C3CH_2), 2.38 (m, 4H, H2'), 1.56–1.47 (m, 4H, H3'), 1.45–1.36 (m, 2H, H4'). ^{13}C NMR (75.4 MHz, acetone- d_6): 136.5, 130.7, 126.3, 124.7, 122.9, 113.9, 113.3, 112.4, 55.2, 55.1, 26.9, 25.4. Anal. Calcd for $\text{C}_{14}\text{H}_{17}\text{BrN}_2$: C, 57.35; H, 5.84; N, 9.55. Found: C, 56.94; H, 5.91; N, 9.32.

1-(1-Benzyl-5-bromo-1H-indol-3-yl)-N,N-dimethylmethanamine (20). Following the general method for the synthesis of **1** derivatives **16–18** and **20–38**, reaction of **2** (97 mg, 0.34 mmol) with dimethylamine (43 μ L, 0.34 mmol) and formaldehyde (25 μ L, 0.34 mmol) in glacial acetic acid (2 mL) yielded **20** as a yellow oil that did not required further purification (114 mg, >99%). ^1H NMR (300 MHz, CDCl_3) δ 7.83 (bd, 1H, J = 1.8 Hz, H4), 7.31–7.19 (m, 4H, Ar), 7.11–7.03

(m, 4H, Ar), 5.24 (s, 2H, NCH₂Ph), 3.55 (s, 2H, C3CH₂), 2.26 [s, 6H, N(CH₃)₂]. Its hydrochloride salt was prepared as described above. Mp 209–212 °C. ¹³C NMR (75.4 MHz, DMSO-*d*₆) δ 137.3, 134.6, 133.5, 129.6, 128.6, 127.6, 127.0, 124.5, 121.6, 112.9, 112.7, 103.0, 50.5, 49.4, 41.1. Anal. Calcd for C₁₈H₁₉BrN₂·HCl: C, 56.94; H, 5.31; N, 7.38. Found: C, 56.53; H, 5.10; N, 7.05.

1-Benzyl-5-bromo-3-(piperidin-1-ylmethyl)-1H-indole (21). Following the general method for the synthesis of **1** derivatives **16–18** and **20–38**, reaction of **2** (138 mg, 0.48 mmol) with piperidine (48 μL, 0.48 mmol) and formaldehyde (35 μL, 0.48 mmol) in glacial acetic acid (0.5 mL) yielded **21** as a yellow oil that did not required further purification (173 mg, 94%). ¹H NMR (300 MHz, CDCl₃) δ 7.86 (d, 1H, *J* = 1.7 Hz, H4), 7.33–7.18 (m, 4H, Ar), 7.10–7.03 (m, 4H, Ar), 5.23 (s, 2H, NCH₂Ph), 3.61 (s, 2H, C3CH₂), 2.42 (m, 4H, H2'), 1.57 (m, 4H, H3'), 1.41 (m, 2H, H4'). Its hydrochloride salt was prepared as described above. Mp 199–202 °C. ¹³C NMR (75.4 MHz, D₂O + few drops of acetone-*d*₆ for ppm calibration) δ 137.3, 135.2, 133.9, 130.2, 129.3, 128.4, 127.4, 125.5, 121.4, 113.9, 113.0, 102.0, 52.5, 51.3, 50.4, 23.2, 21.5. Anal. Calcd for C₂₁H₂₃BrN₂·2HCl: C, 55.28; H, 5.52; N, 6.14. Found: C, 54.92; H, 5.33; N, 6.17.

1-(1-Benzyl-5-methyl-1H-indol-3-yl)-N,N-dimethylmethanamine (22). Following the general method for the synthesis of **1** derivatives **16–18** and **20–38**, reaction of **3** (126 mg, 0.57 mmol) with dimethylamine (72 μL, 0.57 mmol) and formaldehyde (43 μL, 0.57 mmol) in glacial acetic acid (0.6 mL) yielded **22** as a yellow oil that did not required further purification (154 mg, 97%). ¹H NMR (300 MHz, acetone-*d*₆) δ 7.51 (m, 1H, H4), 7.31–7.13 (m, 7H, Ar), 6.94 (dd, 1H, *J* = 1.3, 8.3 Hz, H6), 5.34 (s, 2H, NCH₂Ph), 3.56 (s, 2H, C3CH₂), 2.39 (s, 3H, CH₃), 2.21 [s, 6H, N(CH₂)₃]. Its oxalate salt was prepared as described above. Mp 166–169 °C. ¹³C NMR (75.4

MHz, D₂O + few drops of acetone-*d*₆ for the ppm calibration) δ 215.8, 137.8, 134.8, 132.6, 130.9, 129.2, 128.4, 128.2, 127.3, 124.6, 118.3, 111.1, 102.1, 52.4, 50.2, 41.8, 20.8. **Anal. Calcd for C₁₉H₂₂N₂·2C₂H₂O₄: C, 68.46; H, 6.57; N, 7.60. Found: C, 68.03; H, 6.55; N, 7.25.**

1-Benzyl-5-methyl-3-(piperidin-1-ylmethyl)-1*H*-indole (23). Following the general method for the synthesis of **1** derivatives **16–18** and **20–38**, reaction of **3** (254 mg, 1.15 mmol) with piperidine (113 μ L, 1.15 mmol) and formaldehyde (86 μ L, 1.15 mmol) in glacial acetic acid (2 mL) yielded **23** as a yellow oil that did not required further purification (355 mg, 97%). ¹H NMR (300 MHz, acetone-*d*₆) δ 7.53 (m, 1H, H4), 7.30–7.14 (m, 7H, Ar), 6.93 (dd, 1H, *J* = 1.2, 8.3 Hz, H6), 5.32 (s, 2H, NCH₂Ph), 3.60 (d, 2H, *J* = 0.7 Hz, C3CH₂), 2.44–2.37 (m, 4H, H2'), 2.40 (s, 3H, CH₃), 1.53 (m, 4H, H3'), 1.42 (m, 2H, H4'). Its oxalate salt was prepared as described above. Mp 172–174 °C. ¹³C NMR (75.4 MHz, DMSO-*d*₆) δ 164.6, 137.8, 134.3, 132.0, 128.7, 128.5, 128.4, 127.4, 127.0, 123.5, 118.4, 110.3, 102.1, 51.0, 50.2, 49.3, 22.4, 21.4, 21.1. **Anal. Calcd for C₂₂H₂₆N₂·C₂H₂O₄: C, 70.57; H, 6.91; N, 6.86. Found: C, 70.36; H, 6.86; N, 6.59.**

1-(5-Bromo-1-butyl-1*H*-indol-3-yl)-*N,N*-dimethylmethanamine (24). Following the general method for the synthesis of **1** derivatives **16–18** and **20–38**, reaction of **4** (240 mg, 0.95 mmol) with dimethylamine (120 μ L, 0.95 mmol) and formaldehyde (72 μ L, 0.95 mmol) in glacial acetic acid (1 mL) yielded **24**, which was further purified by automatized flash chromatography with ethyl acetate/hexane mixtures as eluent, obtaining a yellow oil (316 mg, >99%). ¹H NMR (300 MHz, CDCl₃) δ 7.80 (d, 1H, *J* = 1.7 Hz, H4), 7.25 (dd, 1H, *J* = 1.9, 8.7 Hz, H6), 7.16 (d, 1H, *J* = 8.7 Hz, H7), 7.02 (s, 1H, H2), 4.05 (t, 2H, *J* = 7.0 Hz, NCH₂(CH₂)₂CH₃), 3.54 (s, 2H, C3CH₂), 2.25 (s, 6H, N(CH₃)₂), 1.78 (m, 2H, NCH₂CH₂CH₂CH₃), 1.37–1.23 (m, 2H, N(CH₂)₂CH₂CH₃), 0.92 (t, 3H, *J* = 7.3 Hz, CH₃). Its hydrochloride salt was prepared as described above. Mp 84–88

°C. ^{13}C NMR (75.4 MHz, DMSO- d_6) δ 134.6, 133.1, 129.4, 124.3, 121.4, 112.6, 112.4, 102.3, 50.5, 45.5, 41.0, 31.7, 19.3, 13.5. Anal. Calcd for $\text{C}_{15}\text{H}_{21}\text{BrN}_2 \cdot 2\text{HCl}$: C, 47.14; H, 6.07; N, 7.33. Found: C, 46.89; H, 6.38; N, 6.95.

5-Bromo-1-butyl-3-(piperidin-1-ylmethyl)-1*H*-indole (25). Following the general method for the synthesis of **1** derivatives **16–18** and **20–38**, reaction of **4** (185 mg, 0.73 mmol) with piperidine (73 μL , 0.73 mmol) and formaldehyde (66 μL , 0.88 mmol) in glacial acetic acid (0.5 mL) yielded **25** as an oil that did not require further purification (279 mg, >99%). ^1H NMR (300 MHz, CDCl_3) δ 7.83 (d, 1H, $J = 1.8$ Hz, H4), 7.26 (dd, 1H, $J = 1.8, 8.7$ Hz, H6), 7.16 (d, 1H, $J = 8.7$ Hz, H7), 7.03 (s, 1H, H2), 4.04 (t, 2H, $J = 7.1$ Hz, $\text{NCH}_2(\text{CH}_2)_2\text{CH}_3$), 3.62 (s, 2H, C3CH_2), 2.47–2.36 (m, 4H, H2'), 1.79 (m, 2H, $\text{NCH}_2\text{CH}_2\text{CH}_2\text{CH}_3$), 1.58 (m, 4H, H3'), 1.47–1.37 (m, 2H, H4'), 1.37–1.24 (m, 2H, $\text{N}(\text{CH}_2)_2\text{CH}_2\text{CH}_3$), 0.93 (t, 3H, $J = 7.3$ Hz, $\text{N}(\text{CH}_2)_3\text{CH}_3$). Its hydrochloride salt was prepared as described above. Mp 177–180 °C. ^{13}C NMR (75.4 MHz, D_2O + few drops of acetone- d_6 for the ppm calibration) δ 134.8, 133.2, 129.3, 124.8, 120.8, 113.0, 112.4, 100.8, 52.1, 51.1, 46.0, 31.4, 22.8, 21.1, 19.3, 12.8. Anal. Calcd for $\text{C}_{18}\text{H}_{25}\text{BrN}_2 \cdot \text{HCl}$: C, 56.04; H, 6.79; N, 7.26. Found: C, 55.59; H, 6.63; N, 7.08.

1-Butyl-5-methyl-3-(piperidin-1-ylmethyl)-1*H*-indole (26). Following the general method for the synthesis of **1** derivatives **16–18** and **20–38**, reaction of **5** (143 mg, 0.76 mmol) with piperidine (75 μL , 0.76 mmol) and formaldehyde (57 μL , 0.76 mmol) in glacial acetic acid (0.8 mL) yielded **26** as an oil that did not require further purification (204 mg, 94%). ^1H NMR (300 MHz, acetone- d_6) δ 7.50 (m, 1H, H4), 7.25 (d, 1H, $J = 8.3$ Hz, H7), 7.08 (s, 1H, H2), 6.96 (dd, 1H, $J = 1.4, 8.4$ Hz, H6), 4.10 (t, 2H, $J = 7.0$ Hz, $\text{NCH}_2(\text{CH}_2)_2\text{CH}_3$), 3.58 (d, 2H, $J = 0.5$ Hz, C3CH_2), 2.44–2.36 (m, 7H, H2', $\text{CH}_3\text{C5}$), 1.77 (m, 2H, $\text{NCH}_2\text{CH}_2\text{CH}_2\text{CH}_3$), 1.53 (m, 4H, H3'),

1.45–1.35 (m, 2H, H4'), 1.35–1.24 [m, 2H, N(CH₂)₂CH₂CH₃], 0.91 (t, 3H, J = 7.3 Hz, N(CH₂)₃CH₃). Its oxalate salt was prepared as described above. Mp 140–143 °C. ¹³C NMR (75.4 MHz, D₂O + few drops of acetone-*d*₆ for the ppm calibration) δ 134.7, 132.4, 130.5, 128.4, 124.1, 118.2, 110.8, 100.8, 52.3, 51.7, 46.2, 31.8, 23.1, 21.4, 20.8, 19.7, 13.2. **Anal. Calcd for C₁₈H₂₅BrN₂·HCl: C, 56.04; H, 6.79; N, 7.26. Found: C, 55.59; H, 6.63; N, 7.08.**

Ethyl 4-(5-bromo-3-((dimethylamino)methyl)-1*H*-indol-1-yl)butanoate (27). Following the general method for the synthesis of **1** derivatives **16–18** and **20–38**, reaction of **6** (98 mg, 0.32 mmol) with dimethylamine (60 μL, 0.47 mmol) and formaldehyde (34 μL, 0.47 mmol) in glacial acetic acid (1.8 mL) yielded **27** as an oil that did not required further purification (110 mg, 95%). ¹H NMR (300 MHz, acetone-*d*₆) δ 7.86 (d, 1H, J = 1.9 Hz, H4), 7.38 (d, 1H, J = 8.7 Hz, H7), 7.25 (dd, 1H, J = 2.0 Hz, 8.7 Hz, H6), 7.21 (s, 1H, H2), 4.23 [t, 2H, J = 7.0 Hz, NCH₂(CH₂)₂], 4.07 (c, 2H, J = 7.1 Hz, COOCH₂CH₃), 3.53 (s, 2H, C3CH₂), 2.28 (t, 2H, J = 7.8 Hz, CH₂COOCH₂CH₃), 2.18 [s, 6H, N(CH₃)₂], 2.10 (m, 2H, NCH₂CH₂CH₂), 1.19 (t, 3H, J = 7.1 Hz, COOCH₂CH₃). Its oxalate salt was prepared as described above. Mp 133–135 °C. ¹³C NMR (75.4 MHz, CD₃OD) δ 176.3, 165.5, 135.9, 134.0, 130.0, 126.0, 121.7, 114.2, 113.2, 102.6, 62.6, 52.7, 46.5, 42.4, 32.2, 25.6, 14.0. **Anal. Calcd for C₁₇H₂₃BrN₂O₂·H₂O·C₂H₂O₄: C, 48.01; H, 5.73; N, 5.89. Found: C, 48.05; H, 5.31; N, 5.45.**

Ethyl 4-(5-bromo-3-(piperidin-1-ylmethyl)-1*H*-indol-1-yl)butanoate (28). Following the general method for the synthesis of **1** derivatives **16–18** and **20–38**, reaction of **6** (100 mg, 0.32 mmol) with piperidine (48 μL, 0.48 mmol) and formaldehyde (36 μL, 0.48 mmol) in glacial acetic acid (1.1 mL) yielded **28** as an oil that did not required further purification (133 mg, >99%). ¹H NMR (300 MHz, acetone-*d*₆) δ 7.90 (d, 1H, J = 1.9 Hz, H4), 7.38 (d, 1H, J = 8.7 Hz,

H7), 7.25 (dd, 1H, $J = 2.0, 8.7$ Hz, H6), 7.21 (s, 1H, H2), 4.22 [t, 2H, $J = 7.1$ Hz, $\text{NCH}_2(\text{CH}_2)_2\text{CO}$], 4.07 (c, 2H, $J = 7.1$ Hz, $\text{COOCH}_2\text{CH}_3$), 3.58 (s, 2H, C_3CH_2), 2.38 (m, 4H, H2'), 2.28 [t, 2H, $J = 7.1$ Hz, $\text{N}(\text{CH}_2)_2\text{CH}_2\text{CO}$], 2.09 (m, 2H, $\text{NCH}_2\text{CH}_2, \text{CH}_2\text{CO}$), 1.57–1.46 (m, 4H, H3'), 1.46–1.35 (m, 2H, H4'), 1.19 (t, 3H, $J = 7.1$ Hz, $\text{COOCH}_2\text{CH}_3$). Its oxalate salt was prepared as described above. Mp 158–160 °C. ^{13}C NMR (75.4 MHz, CD_3OD) δ 220, 176.0, 136.0, 133.9, 130.5, 126.1, 121.8, 114.4, 113.2, 102.5, 62.4, 53.1, 52.0, 46.5, 32.2, 25.8, 23.8, 22.2, 14.0. Anal. Calcd for $\text{C}_{20}\text{H}_{27}\text{BrN}_2\text{O}_2 \cdot \text{C}_2\text{H}_2\text{O}_4$: C, 53.13; H, 5.88; N, 5.63. Found: C, 53.16; H, 5.85; N, 5.05.

1-(5-Bromo-1-(prop-2-yn-1-yl)-1H-indol-3-yl)-N,N-dimethylmethanamine (29). Following the general method for the synthesis of **1** derivatives **16–18** and **20–38**, reaction of **7** (126 mg, 0.54 mmol) with dimethylamine (68 μL , 0.538 mmol) and formaldehyde (40 μL , 0.54 mmol) in glacial acetic acid (1 mL) yielded **29** as an oil that did not required further purification (154 mg, 98%). ^1H NMR (300 MHz, acetone- d_6) δ 7.88 (d, 1H, $J = 1.9$ Hz, H4), 7.44 (d, 1H, $J = 8.7$ Hz, H7), 7.29 (m, 2H, H6, H2), 5.04 (d, 2H, $J = 2.5$ Hz, NCH_2CCH), 3.53 (s, 2H, C_3CH_2), 2.94 (t, 1H, $J = 2.5$ Hz, NCH_2CCH), 2.19 (s, 6H, $\text{N}(\text{CH}_3)_2$). Its oxalate salt was prepared as described above. Mp 161–163 °C. ^{13}C NMR (75.4 MHz, $\text{DMSO}-d_6$) δ 163.7, 134.4, 132.6, 129.7, 124.8, 121.7, 113.2, 112.7, 103.5, 78.6, 76.4, 50.5, 41.3, 35.6. Anal. Calcd for $\text{C}_{14}\text{H}_{15}\text{BrN}_2 \cdot \text{H}_2\text{O} \cdot 2\text{C}_2\text{H}_2\text{O}_4$: C, 44.19; H, 4.33; N, 5.73. Found: C, 44.15; H, 4.02; N, 5.78.

5-Bromo-3-(piperidin-1-ylmethyl)-1-(prop-2-yn-1-yl)-1H-indole (30). Following the general method for the synthesis of **1** derivatives **16–18** and **20–38**, reaction of **7** (230 mg, 0.98 mmol) with piperidine (97 μL , 0.98 mmol) and formaldehyde (74 μL , 0.98 mmol) in glacial acetic acid (1 mL) yielded **30** as a wax, which did not required further purification (320 mg, 98%). Mp 67–

70 °C. ¹H NMR (300 MHz, acetone-*d*₆) δ 7.91 (d, 1H, *J* = 2.0 Hz, H4), 7.44 (dd, 1H, *J* = 0.4, 8.7 Hz, H7), 7.31–7.27 (m, 2H, H4,H2), 5.04 (d, 2H, *J* = 2.5 Hz, NCH₂CCH), 3.57 (s, 2H, C3CH₂), 2.95 (t, 1H, *J* = 2.5 Hz, NCH₂CCH), 2.38 (m, 4H, H2'), 1.56–1.49 (m, 4H, H3'), 1.44–1.41 (m, 2H, H4'). ¹³C NMR (75.4 MHz, acetone-*d*₆) δ 136.1, 131.4, 129.2, 125.0, 123.3, 113.4, 113.0, 112.4, 79.1, 74.8, 55.1, 54.9, 36.1, 26.9, 25.3. Anal. Calcd for C₁₇H₁₉BrN₂: C, 61.64; H, 5.78; N, 8.46. Found: C, 61.21; H, 5.97; N, 8.60.

***N,N*-Dimethyl-1-(5-methyl-1-(prop-2-yn-1-yl)-1*H*-indol-3-yl)methanamine (31).** Following the general method for the synthesis of **1** derivatives **16–18** and **20–38**, reaction of **8** (236 mg, 1.39 mmol) with dimethylamine (177 μL, 1.39 mmol) and formaldehyde (105 μL, 1.39 mmol) in glacial acetic acid (1.8 mL) yielded **31** as an oil that did not required further purification (282 mg, 90%). ¹H NMR (300 MHz, acetone-*d*₆) δ 7.50 (m, 1H, H4), 7.33 (d, 1H, *J* = 8.3 Hz, H7), 7.17 (s, 1H, H2), 7.02 (dd, 1H, *J* = 1.6, 8.4 Hz, H6), 4.95 (d, 2H, *J* = 2.6 Hz, NCH₂CCH), 3.53 (s, 2H, C3CH₂), 2.90 (t, 1H, *J* = 2.5 Hz, NCH₂CCH), 2.41 (bs, 3H, CH₃C5), 2.19 (s, 6H, N(CH₃)₂). Its oxalate salt was prepared as described above. Mp 136–138 °C. ¹³C NMR (75.4 MHz, D₂O + few drops of acetone-*d*₆ for the ppm calibration) δ 165.0, 134.0, 131.4, 130.9, 128.0, 124.3, 118.0, 110.4, 102.2, 78.3, 74.1, 51.9, 41.5, 35.6, 20.4.

5-Methyl-3-(piperidin-1-ylmethyl)-1-(prop-2-yn-1-yl)-1*H*-indole (32). Following the general method for the synthesis of **1** derivatives **16–18** and **20–38**, reaction of **8** (190 mg, 1.12 mmol) with piperidine (111 μL, 1.12 mmol) and formaldehyde (84 μL, 1.12 mmol) in glacial acetic acid (0.5 mL) yielded **32** as an oil that did not required further purification (287 mg, 96%). ¹H NMR (300 MHz, CDCl₃) δ 7.48 (m, 1H, H4), 7.27 (d, 1H, *J* = 11.6 Hz, H7), 7.13 (s, 1H, H2), 7.07 (dd, 1H, *J* = 2.1, 12.5 Hz, H6), 4.81 (d, 2H, *J* = 3.8 Hz, NCH₂CCH), 3.68 (s, 2H, C3CH₂), 2.86 (s,

1H, NCH₂CCH), 2.57–2.39 (m, 7H, H2', CH₃C5), 1.68–1.51 (m, 4H, H3'), 1.49–1.38 (m, 2H, H4'). Its oxalate salt was prepared as described above. Mp 115–118 °C. ¹³C NMR (75.4 MHz, DMSO-*d*₆) δ 164.1, 134.0, 131.2, 129.0, 128.4, 123.6, 118.5, 110.2, 102.4, 78.8, 76.0, 51.0, 50.1, 35.4, 22.4, 21.4, 21.2.

5-Bromo-1-(4-chlorobutyl)-3-(piperidin-1-ylmethyl)-1*H*-indole (33). Following the general method for the synthesis of **1** derivatives **16–18** and **20–38**, reaction of **9** (311 mg, 1.08 mmol) with piperidine (107 μL, 1.08 mmol) and formaldehyde (81 μL, 1.08 mmol) in glacial acetic acid (0.9 mL) yielded **33**, which was further purified by trituration with diethyl ether, obtaining a yellow oil (419 mg, >99%). ¹H NMR (300 MHz, acetone-*d*₆) δ 7.89 (dd, 1H, *J* = 0.3, 1.9 Hz, H4), 7.38 (d, 1H, *J* = 8.5 Hz, H7), 7.23 (m, 2H, H6, H2), 4.18 [t, 2H, *J* = 6.9 Hz, NCH₂(CH₂)₃Cl], 3.58 (m, 4H, CH₂Cl, C3CH₂), 2.37 (m, 4H, H2'), 2.02–1.70 (m, 4H, NCH₂CH₂CH₂CH₂Cl), 1.56–1.45 (m, 4H, H3'), 1.45–1.35 (m, 2H, H4'). ¹³C NMR (75.4 MHz, DMSO-*d*₆) δ 146.0, 140.8, 139.3, 134.4, 132.9, 122.3, 122.1, 121.9, 64.8, 64.7, 55.7, 54.9, 40.4, 38.1, 36.6, 35.0.

1-(4-Chlorobutyl)-5-methyl-3-(piperidin-1-ylmethyl)-1*H*-indole (34). Following the general method for the synthesis of **1** derivatives **16–18** and **20–38**, reaction of **10** (155 mg, 0.70 mmol) with piperidine (69 μL, 0.70 mmol) and formaldehyde (52 μL, 0.70 mmol) in glacial acetic acid (1.5 mL) yielded **34** as a yellow oil that did not required further purification (229 mg, >99%). ¹H NMR (300 MHz, acetone-*d*₆) δ 7.50 (m, 1H, H4), 7.27 (d, 1H, *J* = 8.4 Hz, H7), 7.09 (s, 1H, H2), 6.97 (dd, 1H, *J* = 1.4, 8.4 Hz, H6), 4.16 [t, 2H, *J* = 6.8 Hz, NCH₂(CH₂)₃Cl], 3.60–3.53 (m, 4H, CH₂Cl, C3CH₂), 2.44–2.33 (m, 4H, H2'), 2.40 (s, 3H, CH₃C5), 1.93 [m, 2H, NCH₂CH₂(CH₂)₂Cl], 1.72 [m, 2H, N(CH₂)₂CH₂CH₂Cl], 1.56–1.47 (m, 4H, H3'), 1.45–1.36 (m,

2H, H4'). Its oxalate salt was prepared as described above. Mp 130–133 °C. ^{13}C NMR (75.4 MHz, DMSO- d_6) δ 164.2, 134.2, 131.3, 128.5, 128.2, 123.4, 121.4, 118.5, 110.1, 51.3, 46.8, 44.9, 44.9, 29.4, 27.2, 24.7, 22.7, 21.2. Anal. Calcd for $\text{C}_{19}\text{H}_{27}\text{ClN}_2 \cdot \text{C}_2\text{H}_2\text{O}_4$: C, 61.68; H, 7.15; N, 6.85. Found: C, 61.60; H, 7.00; N, 6.67.

1-(5-Bromo-1-(4-(piperidin-1-yl)butyl)-1H-indol-3-yl)-N,N-dimethylmethanamine (35).

Following the general method for the synthesis of **1** derivatives **16–18** and **20–38**, reaction of **11** (92 mg, 0.27 mmol) with dimethylamine (35 μL , 0.27 mmol) and formaldehyde (21 μL , 0.27 mmol) in glacial acetic acid (1.8 mL) yielded **35** as an oil that did not required further purification (115 mg, >99%). ^1H NMR (300 MHz, acetone- d_6) δ 7.85 (d, 1H, J = 2.0 Hz, H4), 7.39 (d, 1H, J = 8.7 Hz, H7), 7.23 (m, 2H, H6, H2), 4.18 [t, 2H, J = 7.1 Hz, $\text{NCH}_2(\text{CH}_2)_3\text{N}$], 3.52 (s, 2H, C_3CH_2), 2.30–2.19 [m, 6H, $\text{N}(\text{CH}_2)_3\text{CH}_2\text{N}$, H2'], 2.17 [s, 6H, $\text{N}(\text{CH}_3)_2$], 1.83 [m, 2H, $\text{NCH}_2\text{CH}_2(\text{CH}_2)_2\text{N}$], 1.53–1.32 [m, 8H, $\text{N}(\text{CH}_2)_2\text{CH}_2\text{CH}_2\text{N}$, H3', H4']. Its oxalate salt was prepared as described above. Mp 123–125 °C. ^{13}C NMR (75.4 MHz, D_2O + few drops of acetone- d_6 for ppm calibration) δ 165.7, 135.2, 133.2, 129.4, 125.5, 121.2, 113.6, 112.6, 102.1, 56.5, 53.3, 52.1, 45.9, 41.8, 26.8, 23.0, 21.4, 21.2. Anal. Calcd for $\text{C}_{20}\text{H}_{30}\text{BrN}_3 \cdot \text{H}_2\text{O} \cdot 2\text{C}_2\text{H}_2\text{O}_4$: C, 48.82; H, 6.15; N, 7.12. Found: C, 49.26; H, 6.04; N, 6.75.

5-Bromo-1-(4-(piperidin-1-yl)butyl)-3-(piperidin-1-ylmethyl)-1H-indole (36). Following the

general method for the synthesis of **1** derivatives, reaction of **11** (70 mg, 0.21 mmol) with piperidine (21 μL , 0.21 mmol) and formaldehyde (16 μL , 0.21 mmol) in glacial acetic acid (400 μL) yielded **36** as an oil that did not required further purification (90 mg, >99%). ^1H NMR (300 MHz, acetone- d_6) δ 7.99 (d, 1H, J = 1.8 Hz, H4), 7.37 (d, 1H, J = 8.7 Hz, H7), 7.22 (dd, 1H, J_{4-6} = 1.8, 8.7 Hz, H6), 7.19 (s, 1H, H2), 4.16 [t, 2H, J = 7.1 Hz, $\text{NCH}_2(\text{CH}_2)_3\text{N}$], 3.56 (s, 2H,

C3CH₂), 2.37 (m, 4H, H2''), 2.29–2.18 [m, 6H, N(CH₂)₃CH₂N, H2'], 1.83 [m, 2H, NCH₂CH₂(CH₂)₂N], 1.55–1.34 [m, 14H, N(CH₂)₂CH₂CH₂N, H3', H4', H3'', H4'']. Its oxalate salt was prepared as described above. Mp 90–92 °C. ¹³C NMR (75.4 MHz, D₂O + few drops of acetone-*d*₆ for the ppm calibration) δ 168.2, 135.1, 133.3, 129.8, 125.4, 121.4, 113.7, 112.6, 101.8, 56.5, 53.3, 52.5, 51.4, 45.9, 26.8, 23.2, 23.0, 21.5, 21.2. Anal. Calcd for C₂₃H₃₄BrN₃·2C₂H₂O₄: C, 52.94; H, 6.25; N, 6.86. Found: C, 52.89; H, 6.67; N, 6.86.

***N,N*-Dimethyl-1-(5-methyl-1-(4-(piperidin-1-yl)butyl)-1*H*-indol-3-yl)methanamine (37).**

Following the general method for the synthesis of **1** derivatives, reaction of **12** (93 mg, 0.34 mmol) with dimethylamine (44 μL, 0.34 mmol) and formaldehyde (26 μL, 0.34 mmol) in glacial acetic acid (0.6 mL) yielded **37** as a yellow oil that did not required further purification (102 mg, 91%). ¹H NMR (300 MHz, acetone-*d*₆) δ 7.46 (m, 1H, H4), 7.28 (d, 1H, *J* = 8.3 Hz, H7), 7.11 (s, 1H, H2), 6.96 (dd, 1H, *J* = 1.5, 8.3 Hz, H6), 4.13 [t, 2H, *J* = 7.0 Hz, NCH₂(CH₂)₃N], 3.53 (s, 2H, C3CH₂), 2.40 (s, 3H, CH₃C5), 2.31–2.20 [m, 6H, N(CH₂)₃CH₂N, H2'], 2.18 [s, 6H, N(CH₃)₂], 1.82 [m, 2H, NCH₂CH₂(CH₂)₂N], 1.54–1.44 (m, 4H, H3'), 1.44–1.34 (m, 2H, H4'). Its oxalate salt was prepared as described above. Mp 146–149 °C. ¹³C NMR (75.4 MHz, DMSO-*d*₆) δ 164.6, 134.1, 131.6, 128.6, 128.1, 123.4, 118.4, 110.1, 102.3, 55.3, 52.0, 50.9, 45.1, 41.2, 26.7, 22.4, 21.4, 21.2, 20.7. Anal. Calcd for C₂₁H₃₅N₃·H₂O 2C₂H₂O₄: C, 57.13; H, 7.48; N, 7.99. Found: C, 57.49; H, 7.11; N, 7.61.

5-Methyl-1-(4-(piperidin-1-yl)butyl)-3-(piperidin-1-ylmethyl)-1*H*-indole (38). Following the general method for the synthesis of **1** derivatives, reaction of **12** (120 mg, 0.44 mmol) with piperidine (44 μL, 0.44 mmol) and formaldehyde (33 μL, 0.444 mmol) in glacial acetic acid (1.8 mL) yielded **38** as an oil that did not required further purification (162 mg, 96%). ¹H NMR (300

MHz, acetone- d_6) δ 7.48 (m, 1H, H4), 7.27 (m, 1H, H7), 7.07 (s, 1H, H2), 6.95 (dd, 1H, $J = 2.1$, 12.3 Hz, H6), 4.11 [t, 2H, $J = 10.4$ Hz, $\text{NCH}_2(\text{CH}_2)_3\text{N}$], 3.56 (d, 2H, $J = 1.0$ Hz, C3CH_2), 2.44-2.32 (m, 7H, $\text{H2}''$, $\text{CH}_3\text{C5}$), 2.30–2.16 [m, 6H, $\text{N}(\text{CH}_2)_3\text{CH}_2\text{N}$, $\text{H2}'$], 1.80 [m, 2H, $\text{NCH}_2\text{CH}_2(\text{CH}_2)_2\text{N}$], 1.59–1.33 [m, 14H, $\text{N}(\text{CH}_2)_2\text{CH}_2\text{CH}_2\text{N}$, $\text{H3}'$, $\text{H4}'$, $\text{H3}''$, $\text{H4}''$]. Its oxalate salt was prepared as described above. Mp 64–66 °C. ^{13}C NMR (75.4 MHz, DMSO - d_6) δ 164.2, 134.0, 131.7, 128.6, 128.4, 123.4, 118.4, 110.1, 101.7, 55.4, 52.1, 51.3, 50.5, 45.1, 26.6, 22.5, 22.5, 21.4, 21.4, 21.2, 20.8. . Anal. Calcd for $\text{C}_{24}\text{H}_{37}\text{N}_3 \cdot \text{H}_2\text{O} \cdot 2\text{C}_2\text{H}_2\text{O}_4$: C, 59.45; H, 7.66; N, 7.43. Found: C, 59.82; H, 7.36; N, 7.18.

Molecular Modeling. The structure and conformational analysis of ligand **23** were obtained with the Monte Carlo method in Spartan10. The most stable conformer were subsequently optimized with ab initio Hartree-Fock 6-31G* calculations, and selected for docking studies. The 3D structure of the Protein Phosphatase 2A bound to OA was obtained from the Protein Data Bank (PDB ID: 2IE4).⁷⁰ All solvent molecules and the co-crystallized ligand okadaic acid were removed from the complex. Molecular docking calculations for PP2A and compound **23** were undertaken using Molegro Virtual Docker 3.0,⁹³ under a large enough sphere able to accommodate the cavity, centering it on the binding site of the protein structure, to allow the ligand to search the best pose. Different orientations of the ligands were searched and ranked based on their energy scores. Poses with the best both energies and conformations were selected for further 3D analysis. MolDock Score was used as algorithm, which is adapted from the Differential Evolution (DE) algorithm.

Pharmacology. Data Analysis. Data are shown as means \pm standard error of the mean (SEM). Statistical significant differences ($p \leq 0.05$) were calculated by ANOVA followed by a Newman-Keuls or Dunnett's post hoc test, obtained using the Prism software 5.0 (GraphPad) for a Mac OS X-operated computer.

Experimental Use of Animals. All efforts were made to minimize the number of animals used for the experiments and their suffering. We followed the guidelines of the EU Council Directive. Experiments were approved by the Ethics Committee of the Universidad Autónoma de Madrid, Spain.

Culture and treatment of neuroblastoma cells. SH-SY5Y cells were maintained similarly to what was previously described.⁶³ For neuroprotection assays, cells were subcultured in 48 well plates at a seeding density of 7×10^4 cells per well. Before cells achieved confluence, compounds dissolved in media supplemented with 10% fetal bovine serum (FBS) were preincubated for 24 h. For coincubation, media was replaced by fresh new media with 1% FBS, compounds and the corresponding toxic stimulus. When coincubation finished, cell viability or phosphatase activities were measured.

Culture and treatment of rat hippocampal slices. Hippocampal slices from 2-month-old Sprague-Dawley rats were extracted, isolated, and treated with glutamate according to experimental procedures previously described.⁵¹ After stabilization at 34 °C for 45 min, compounds and glutamate dissolved in water were coincubated for 4 h and cell viability was measured by the method of the MTT reduction.

Culture and treatment of rat motor cortical neurons. Embryos from 18 to 19 days of pregnancy were obtained by caesarean operation. After decapitation of the embryos and

dissection of the brains, meninges were removed and the motor cortex was isolated. The fragments obtained from several embryos were subjected to mechanic digestion. Motor cortical neurons were resuspended in Neurobasal medium with 2% B-27 and seeded in poly-*D*-lysine-pre-coated 48-well plates (density of 3×10^4 cells per well). Neuronal cultures were allowed to grow 8 to 10 days until a dense neuronal network was observed. Tested compounds dissolved in medium were preincubated for 24 h, after which veratridine was directly added into the wells and allowed to coincubate for another 24 h. The cell viability was assessed by the method of the MTT reduction.

Measurement of cell viability in SH-SY5Y cells, hippocampal slices and motor cortex neurons. Cell viability was assessed by the quantitative colorimetric method of the MTT reduction.⁷⁶ Briefly, only in living cells the MTT (3-[4,5-dimethylthiazol-2-yl]-2,5-diphenyltetrazolium bromide, yellow-colored) is chemically reduced by mitochondrial dehydrogenase enzymes, thus being cell viability indirectly measured as mitochondrial activity of healthy cells. The reduced MTT is a purple-colored formazan derivative, which is dissolved in DMSO and offers a concentration-dependent colorimetric signal at 540 nm. MTT dissolved in water at 10 mg/mL was added to the wells (final concentration of 0.3 mg/mL) and was incubated in the dark at 37 °C for 2 h or 30 min depending on SH-SY5Y cells or hippocampal slices and neurons, respectively. After harvesting the medium, cells and tissue were lysed and the formazan dissolved with 300 µL, 200 µL or 120 µL of DMSO, as if it is SH-SY5Y cells, hippocampal slices or neurons. Absorbance was measured at 540 nm in a colorimetric plate reader (FLUOstar Optima, BMG, Germany). Data were expressed as percentage of cell viability, taking as 100% the obtained absorbance value in untreated cells.

Measurement of phosphatase activity in SH-SY5Y cells. The Biosciences Phosphatase Assay Kit (Cat. #786-453) was used to measure the activity of phosphatases. Briefly, *p*-nitrophenyl phosphate (pNPP) acts as chromogenic substrate for the phosphatases, generating *p*-nitrophenol when dephosphorylated, which is deprotonated under alkaline conditions to produce *p*-nitrophenolate that has a strong absorption at 405 nm. For total phosphatase activity, cellular media was removed and 50 μ L of assay buffer and substrate (10 mM) were added to each well. The reaction mixture was incubated in the dark at 37 °C for 30 min and the absorbance was measured at 405 nm (FLUOstar Optima, BMG, Germany). Ser/Thr phosphatase activity was measured by adding NaVO₃ 1mM to the buffer. Data were reported as percentage of phosphatase activity, taking as 100% the obtained absorbance value in untreated cells.

Measurement of cytosolic Ca²⁺ in SH-SY5Y cells. Free cytosolic Ca²⁺ was measured using the fluorescent Ca²⁺ indicator Fluo-4/AM (Fluo-4 acetomethoxyester). SH-SY5Y cells were seeded onto 96-well black plates at a density of 10⁵ cells per well, achieving confluence after 48 h. Cells were washed with Krebs-Hepes solution (KH, in mM: 144 NaCl, 5.9 KCl, 1.2 MgCl₂, 2 CaCl₂, 11 D-glucose, 10 HEPES, pH 7.4). Cells were loaded with 10 μ M Fluo-4/AM and 0.2% pluronic acid in KH and incubated for 45 min at 37 °C in the dark. Then, cells were washed twice with KH to remove the excess of probe. Tested compounds were incubated 10 min before K⁺ 70 mM was applied to evoke the increment of cytosolic Ca²⁺. To normalize Fluo-4 signals, Triton X-100 (5%) and 1 M MnCl₂ were applied to register both maximal and minimal fluorescence, respectively. The experiments were analyzed at excitation and emission wavelengths of 485 and 520 nm, respectively, and fluorescence was measured in a fluorescence microplate reader (FLUOstar Optima, BMG, Germany). Data were calculated as a percentage of $F_{\max} - F_{\min}$.

Culture and measurement of Ca^{2+} currents in chromaffin cells. Bovine chromaffin cells were isolated and cultured according to a protocol previously described.⁹⁴ All experiments were performed at room temperature (26 ± 2 °C) on cells from 1 to 4 days after culture. I_{Ca} were measured under the whole cell configuration of the patch-clamp technique.⁹⁵ During recording, cells were constantly perfused with a standard control solution at pH 7.4 containing (mM): 145 NaCl, 5.6 KCl, 1.2 MgCl_2 , 2 CaCl_2 , 11 glucose and 10 HEPES/NaOH. Cells were internally dialysed with an intracellular solution containing (in mM): 100 Cs-glutamate, 14 EGTA, 20 tetraethylammonium, 10 NaCl, 5 ATP-Mg, 0.3 GTP-Na, and 20 HEPES/CsOH (pH 7.3). Whole-cell recordings were made with fire-polished borosilicate pipettes (resistance 2-5 M Ω) that were mounted on the headstage of an EPC-9 patch-clamp amplifier (HEKA Elektronik, Lambrecht, Germany), allowing cancellation of capacitative transients and compensation of series resistance. Data were recorded in a frequency of 20 kHz by using PULSE v8.74 software (HEKA Elektronik). Data analyses were performed with PULSE v8.74 program (HEKA Elektronik). Coverslips containing the cells were placed on a chamber installed on the stage of a inverted microscope. The external solutions were exchanged using miniature solenoid valves coupled to a multi-barrel concentration clamp apparatus, placing the common outlet within the 100 μm of the cell to be patched. The flow rate was 1 mL/min and was regulated by gravity. Nifedipine and different compounds were perfused as indicated. In order to measure I_{Ca} , cells were stabilized at -80 mV and, each 20-s, single depolarizing pulses were applied to voltages where I_{Ca} peak was reached.

ANCILLARY INFORMATION

Supporting Information

^1H NMR spectra of compounds **2–38** and ^{13}C NMR spectra of tested compounds **15–38**, scheme of patch-clamp experimental protocols, in vitro toxicity experiments with the tested compounds. This material is available free of charge via the Internet at <http://pubs.acs.org>.

Corresponding Authors

*For C.d.I.R.: phone, +34-914972765; fax, +34-914973453; E-mail, cristobal.delosrios@inv.uam.es

Present Addresses

^{||}Instituto de Investigación Sanitaria, Fundación Jiménez Díaz, Universidad Autónoma de Madrid, Avda. Reyes Católicos, 2, 28040 Madrid, Spain.

ACKNOWLEDGMENTS

This work was supported by the following grant: Proyectos de Investigación en Salud (PI13/00789, IS Carlos III). R.L.C is granted by Universidad Autónoma de Madrid. We thank the continued support of Fundación de Investigación Biomédica, Hospital Universitario de la Princesa, and Fundación Teófilo Hernando.

ABBREVIATIONS USED

A β , amyloid β peptide ; AD, Alzheimer's disease; ChE, cholinesterases; I_{Ca}, Ca²⁺ currents; I/V, current vs. voltage; MTT, 3-(4,5-dimethylthiazol-2-yl)-2,5-diphenyltetrazolium bromide; NFT, neurofibrillary tangles; NMDA, *N*-methyl-*D*-aspartate; OA, okadaic acid; *p*NPP, *p*-nitrophenylphosphate; PP1, phosphoprotein phosphatase 1; PP2A, phosphoprotein phosphatase 2A; PPP, phosphoprotein phosphatases; TTX, tetrodotoxin; VGCC, voltage-gated Ca²⁺ channels; VGNC, voltage-gated Na⁺ channels; ω -ctx, ω -conotoxin.

References

- (1) Alzheimer, A. Über einen eigenartige erkrankung der hirnrinde. *Alleomag. Z. Psych.* **1907**, *64*, 146–148.
- (2) Scheltens, P.; Blennow, K.; Breteler, M. M.; de Strooper, B.; Frisoni, G. B.; Salloway, S.; Van der Flier, W. M. Alzheimer's disease. *Lancet* **2016**, DOI: 10.1016/S0140-6736(15)01124-1
- (3) Anand, R.; Gill, K. D.; Mahdi, A. A. Therapeutics of Alzheimer's disease: Past, present and future. *Neuropharmacology* **2014**, *76 Pt A*, 27–50.
- (4) Mullard, A. Sting of Alzheimer's failures offset by upcoming prevention trials. *Nat. Rev. Drug Discovery* **2012**, *11*, 657–660.
- (5) Herrup, K. The case for rejecting the amyloid cascade hypothesis. *Nat. Neurosci.* **2015**, *18*, 794–799.
- (6) Iqbal, K.; Liu, F.; Gong, C. X. Tau and neurodegenerative disease: the story so far. *Nat. Rev. Neurol.* **2016**, *12*, 15–27.

- (7) Salahuddin, P.; Fatima, M. T.; Abdelhameed, A. S.; Nusrat, S.; Khan, R. H. Structure of amyloid oligomers and their mechanisms of toxicities: Targeting amyloid oligomers using novel therapeutic approaches. *Eur. J. Med. Chem.* **2016**, *114*, 41–58.
- (8) Bulic, B.; Pickhardt, M.; Mandelkow, E. M.; Mandelkow, E. Tau protein and tau aggregation inhibitors. *Neuropharmacology* **2010**, *59*, 276–289.
- (9) Gong, C. X.; Iqbal, K. Hyperphosphorylation of microtubule-associated protein tau: a promising therapeutic target for Alzheimer disease. *Curr. Med. Chem.* **2008**, *15*, 2321–2328.
- (10) Carreiras, M. C.; Mendes, E.; Perry, M. J.; Francisco, A. P.; Marco-Contelles, J. The multifactorial nature of Alzheimer's disease for developing potential therapeutics. *Curr. Top. Med. Chem.* **2013**, *13*, 1745–1770.
- (11) Guzior, N.; Wieckowska, A.; Panek, D.; Malawska, B. Recent development of multifunctional agents as potential drug candidates for the treatment of Alzheimer's disease. *Curr. Med. Chem.* **2015**, *22*, 373–404.
- (12) Fang, L.; Appenroth, D.; Decker, M.; Kiehnopf, M.; Lupp, A.; Peng, S.; Fleck, C.; Zhang, Y.; Lehmann, J. NO-donating tacrine hybrid compounds improve scopolamine-induced cognition impairment and show less hepatotoxicity. *J. Med. Chem.* **2008**, *51*, 7666–7669.
- (13) Simoni, E.; Serafini, M. M.; Bartolini, M.; Caporaso, R.; Pinto, A.; Necchi, D.; Fiori, J.; Andrisano, V.; Minarini, A.; Lanni, C.; Rosini, M. Nature-inspired multifunctional ligands: focusing on amyloid-based molecular mechanisms of Alzheimer's disease. *ChemMedChem* **2016**, DOI: 10.1002/cmdc.201500422.
- (14) Di Martino, R. M.; De Simone, A.; Andrisano, V.; Bisignano, P.; Bisi, A.; Gobbi, S.; Rampa, A.; Fato, R.; Bergamini, C.; Perez, D. I.; Martinez, A.; Bottegoni, G.; Cavalli, A.;

Belluti, F. Versatility of the curcumin scaffold: discovery of potent and balanced dual BACE-1 and GSK-3 β inhibitors. *J. Med. Chem.* **2016**, *59*, 531–544.

(15) Bolea, I.; Juarez-Jimenez, J.; de Los Rios, C.; Chioua, M.; Pouplana, R.; Luque, F. J.; Unzeta, M.; Marco-Contelles, J.; Samadi, A. Synthesis, biological evaluation, and molecular modeling of donepezil and N-[(5-(benzyloxy)-1-methyl-1H-indol-2-yl)methyl]-N-methylprop-2-yn-1-amine hybrids as new multipotent cholinesterase/monoamine oxidase inhibitors for the treatment of Alzheimer's disease. *J. Med. Chem.* **2011**, *54*, 8251–8270.

(16) Romero, A.; Egea, J.; Gonzalez-Munoz, G. C.; Martin de Saavedra, M. D.; del Barrio, L.; Rodriguez-Franco, M. I.; Conde, S.; Lopez, M. G.; Villarroya, M.; de los Rios, C. ITH12410/SC058: a new neuroprotective compound with potential in the treatment of Alzheimer's disease. *ACS Chem. Neurosci.* **2014**, *5*, 770–775.

(17) Martinez-Sanz, F. J.; Lajarin-Cuesta, R.; Moreno-Ortega, A. J.; Gonzalez-Lafuente, L.; Fernandez-Morales, J. C.; Lopez-Arribas, R.; Cano-Abad, M. F.; de los Rios, C. Benzothiazepine CGP37157 analogues exert cytoprotection in various in vitro models of neurodegeneration. *ACS Chem. Neurosci.* **2015**, *6*, 1626–1636.

(18) Egea, J.; de los Rios, C. 1,8-Naphthyridine derivatives as cholinesterases inhibitors and cell Ca²⁺ regulators, a multitarget strategy for Alzheimer's disease. *Curr. Top. Med. Chem.* **2011**, *11*, 2807–2823.

(19) Samadi, A.; Valderas, C.; de los Rios, C.; Bastida, A.; Chioua, M.; Gonzalez-Lafuente, L.; Colmena, I.; Gandia, L.; Romero, A.; Del Barrio, L.; Martin-de-Saavedra, M. D.; Lopez, M. G.; Villarroya, M.; Marco-Contelles, J. Cholinergic and neuroprotective drugs for the treatment of Alzheimer and neuronal vascular diseases. II. Synthesis, biological assessment, and molecular

modelling of new tacrine analogues from highly substituted 2-aminopyridine-3-carbonitriles.

Bioorg. Med. Chem. **2011**, *19*, 122–133.

(20) Zundorf, G.; Reiser, G. Calcium dysregulation and homeostasis of neural calcium in the molecular mechanisms of neurodegenerative diseases provide multiple targets for neuroprotection. *Antioxid. Redox Signaling* **2011**, *14*, 1275–1288.

(21) Riascos, D.; Nicholas, A.; Samaeekia, R.; Yukhananov, R.; Mesulam, M. M.; Bigio, E. H.; Weintraub, S.; Guo, L.; Geula, C. Alterations of Ca(2)(+)-responsive proteins within cholinergic neurons in aging and Alzheimer's disease. *Neurobiol. Aging* **2014**, *35*, 1325–1333.

(22) Resende, R.; Pereira, C.; Agostinho, P.; Vieira, A. P.; Malva, J. O.; Oliveira, C. R. Susceptibility of hippocampal neurons to Abeta peptide toxicity is associated with perturbation of Ca²⁺ homeostasis. *Brain Res.* **2007**, *1143*, 11–21.

(23) Mark, R. J.; Hensley, K.; Butterfield, D. A.; Mattson, M. P. Amyloid beta-peptide impairs ion-motive ATPase activities: evidence for a role in loss of neuronal Ca²⁺ homeostasis and cell death. *J. Neurosci.* **1995**, *15*, 6239–6249.

(24) Fernandez-Morales, J. C.; Arranz-Tagarro, J. A.; Calvo-Gallardo, E.; Maroto, M.; Padin, J. F.; Garcia, A. G. Stabilizers of neuronal and mitochondrial calcium cycling as a strategy for developing a medicine for Alzheimer's disease. *ACS Chem. Neurosci.* **2012**, *3*, 873–883.

(25) Nimmrich, V.; Eckert, A. Calcium channel blockers and dementia. *Br. J. Pharmacol.* **2013**, *169*, 1203–1210.

(26) Zamponi, G. W. Targeting voltage-gated calcium channels in neurological and psychiatric diseases. *Nat. Rev. Drug Discovery* **2016**, *15*, 19–34.

- (27) Asakura, K.; Matsuo, Y.; Kanemasa, T.; Ninomiya, M. P/Q-type Ca²⁺ channel blocker omega-agatoxin IVA protects against brain injury after focal ischemia in rats. *Brain Res.* **1997**, *776*, 140–145.
- (28) Berman, R. F.; Verweij, B. H.; Muizelaar, J. P. Neurobehavioral protection by the neuronal calcium channel blocker ziconotide in a model of traumatic diffuse brain injury in rats. *J. Neurosurg.* **2000**, *93*, 821–828.
- (29) Hosaka, T.; Yamamoto, Y. L.; Diksic, M. Efficacy of retrograde perfusion of the cerebral vein with verapamil after focal ischemia in rat brain. *Stroke* **1991**, *22*, 1562–1566.
- (30) Paris, D.; Bachmeier, C.; Patel, N.; Quadros, A.; Volmar, C. H.; Laporte, V.; Ganey, J.; Beaulieu-Abdelahad, D.; Ait-Ghezala, G.; Crawford, F.; Mullan, M. J. Selective antihypertensive dihydropyridines lower Abeta accumulation by targeting both the production and the clearance of Abeta across the blood-brain barrier. *Mol. Med.* **2011**, *17*, 149–162.
- (31) Lopez-Arrieta, J. M.; Birks, J. Nimodipine for primary degenerative, mixed and vascular dementia. *Cochrane Database Syst. Rev.* **2002**, CD000147.
- (32) Lajarin-Cuesta, R.; Arribas, R. L.; De Los Rios, C. Ligands for Ser/Thr phosphoprotein phosphatases: a patent review (2005-2015). *Expert Opin. Ther. Pat.* **2016**, *26*, 389–407.
- (33) Tell, V.; Hilgeroth, A. Recent developments of protein kinase inhibitors as potential AD therapeutics. *Front. Cell. Neurosci.* **2013**, *7*, 189.
- (34) Lovestone, S.; Boada, M.; Dubois, B.; Hull, M.; Rinne, J. O.; Huppertz, H. J.; Calero, M.; Andres, M. V.; Gomez-Carrillo, B.; Leon, T.; del Ser, T. A phase II trial of tideglusib in Alzheimer's disease. *J. Alzheimer's Dis.* **2015**, *45*, 75–88.

- (35) Zhang, M.; Yogesha, S. D.; Mayfield, J. E.; Gill, G. N.; Zhang, Y. Viewing serine/threonine protein phosphatases through the eyes of drug designers. *FEBS J.* **2013**, *280*, 4739–4760.
- (36) Liu, F.; Grundke-Iqbal, I.; Iqbal, K.; Gong, C. X. Contributions of protein phosphatases PP1, PP2A, PP2B and PP5 to the regulation of tau phosphorylation. *Eur. J. Neurosci.* **2005**, *22*, 1942–1950.
- (37) Gong, C. X.; Liu, F.; Wu, G.; Rossie, S.; Wegiel, J.; Li, L.; Grundke-Iqbal, I.; Iqbal, K. Dephosphorylation of microtubule-associated protein tau by protein phosphatase 5. *J. Neurochem.* **2004**, *88*, 298–310.
- (38) Vogelsberg-Ragaglia, V.; Schuck, T.; Trojanowski, J. Q.; Lee, V. M. PP2A mRNA expression is quantitatively decreased in Alzheimer's disease hippocampus. *Exp. Neurol.* **2001**, *168*, 402–412.
- (39) Sontag, E.; Luangpirom, A.; Hladik, C.; Mudrak, I.; Ogris, E.; Speciale, S.; White, C. L., 3rd. Altered expression levels of the protein phosphatase 2A AB α C enzyme are associated with Alzheimer disease pathology. *J. Neuropathol. Exp. Neurol.* **2004**, *63*, 287–301.
- (40) Tanimukai, H.; Grundke-Iqbal, I.; Iqbal, K. Up-regulation of inhibitors of protein phosphatase-2A in Alzheimer's disease. *Am. J. Pathol.* **2005**, *166*, 1761–1771.
- (41) Chen, S.; Li, B.; Grundke-Iqbal, I.; Iqbal, K. I β PP2A affects tau phosphorylation via association with the catalytic subunit of protein phosphatase 2A. *J. Biol. Chem.* **2008**, *283*, 10513–10521.
- (42) Longin, S.; Zwaenepoel, K.; Louis, J. V.; Dilworth, S.; Goris, J.; Janssens, V. Selection of protein phosphatase 2A regulatory subunits is mediated by the C terminus of the catalytic Subunit. *J. Biol. Chem.* **2007**, *282*, 26971–26980.

- (43) Sontag, E.; Hladik, C.; Montgomery, L.; Luangpirom, A.; Mudrak, I.; Ogris, E.; White, C. L., 3rd. Downregulation of protein phosphatase 2A carboxyl methylation and methyltransferase may contribute to Alzheimer disease pathogenesis. *J. Neuropathol. Exp. Neurol.* **2004**, *63*, 1080–1091.
- (44) Drewes, G.; Mandelkow, E. M.; Baumann, K.; Goris, J.; Merlevede, W.; Mandelkow, E. Dephosphorylation of tau protein and Alzheimer paired helical filaments by calcineurin and phosphatase-2A. *FEBS Lett.* **1993**, *336*, 425–432.
- (45) Sontag, E.; Nunbhakdi-Craig, V.; Lee, G.; Brandt, R.; Kamibayashi, C.; Kuret, J.; White, C. L., 3rd; Mumby, M. C.; Bloom, G. S. Molecular interactions among protein phosphatase 2A, tau, and microtubules. Implications for the regulation of tau phosphorylation and the development of tauopathies. *J. Biol. Chem.* **1999**, *274*, 25490–25498.
- (46) Gong, C. X.; Grundke-Iqbal, I.; Iqbal, K. Dephosphorylation of Alzheimer's disease abnormally phosphorylated tau by protein phosphatase-2A. *Neuroscience* **1994**, *61*, 765–772.
- (47) Ma, O. K.; Sucher, N. J. Molecular interaction of NMDA receptor subunit NR3A with protein phosphatase 2A. *Neuroreport* **2004**, *15*, 1447–1450.
- (48) Zhu, M.; Wang, J.; Liu, M.; Du, D.; Xia, C.; Shen, L.; Zhu, D. Upregulation of protein phosphatase 2A and NR3A-pleiotropic effect of simvastatin on ischemic stroke rats. *PLoS One* **2012**, *7*, e51552.
- (49) Martin, L.; Latypova, X.; Wilson, C. M.; Magnaudeix, A.; Perrin, M. L.; Yardin, C.; Terro, F. Tau protein kinases: involvement in Alzheimer's disease. *Ageing Res. Rev.* **2013**, *12*, 289–309.
- (50) de Los Rios, C.; Egea, J.; Marco-Contelles, J.; Leon, R.; Samadi, A.; Iriepa, I.; Moraleda, I.; Galvez, E.; Garcia, A. G.; Lopez, M. G.; Villarroja, M.; Romero, A. Synthesis, inhibitory

activity of cholinesterases, and neuroprotective profile of novel 1,8-naphthyridine derivatives. *J. Med. Chem.* **2010**, *53*, 5129–5143.

(51) Lorrio, S.; Romero, A.; Gonzalez-Lafuente, L.; Lajarin-Cuesta, R.; Martinez-Sanz, F. J.; Estrada, M.; Samadi, A.; Marco-Contelles, J.; Rodriguez-Franco, M. I.; Villarroya, M.; Lopez, M. G.; de los Rios, C. PP2A ligand ITH12246 protects against memory impairment and focal cerebral ischemia in mice. *ACS Chem. Neurosci.* **2013**, *4*, 1267–1277.

(52) Settimo, A. D.; Primofiore, G.; Ferrarini, P. L. Bromoderivatives of gramines. Preparation and pharmacological properties. *Eur. J. Med. Chem.* **1983**, *18*, 261–267.

(53) Iwata, S.; Saito, S.; Kon-ya, K.; Shizuri, Y.; Ohizumi, Y. Novel marine-derived halogen-containing gramine analogues induce vasorelaxation in isolated rat aorta. *Eur. J. Pharmacol.* **2001**, *432*, 63–70.

(54) Pelech, S.; Cohen, P. The protein phosphatases involved in cellular regulation. 1. Modulation of protein phosphatases-1 and 2A by histone H1, protamine, polylysine and heparin. *Eur. J. Biochem.* **1985**, *148*, 245–251.

(55) Voronkov, M.; Braithwaite, S. P.; Stock, J. B. Phosphoprotein phosphatase 2A: a novel druggable target for Alzheimer's disease. *Future Med. Chem.* **2011**, *3*, 821–833.

(56) Lambrecht, C.; Haesen, D.; Sents, W.; Ivanova, E.; Janssens, V. Structure, regulation, and pharmacological modulation of PP2A phosphatases. *Methods Mol. Biol.* **2013**, *1053*, 283–305.

(57) Gurer-Orhan, H.; Suzen, S. Melatonin, its metabolites and its synthetic analogs as multi-faceted compounds: antioxidant, prooxidant and inhibitor of bioactivation reactions. *Curr. Med. Chem.* **2015**, *22*, 490–499.

(58) Aiello, F.; Valacchi, G. Synthesis and evaluation of indole based molecules for treatment of oxidative stress related diseases. *Curr. Top. Med. Chem.* **2014**, *14*, 2576–2589.

- (59) Camacho, M. E.; Carrion, M. D.; Lopez-Cara, L. C.; Entrena, A.; Gallo, M. A.; Espinosa, A.; Escames, G.; Acuna-Castroviejo, D. Melatonin synthetic analogs as nitric oxide synthase inhibitors. *Mini Rev. Med. Chem.* **2012**, *12*, 600–617.
- (60) Semenov, B. B.; Granik, V. G. Chemistry of N-(1H-indol-3-ylmethyl)-N,N-dimethylamine (Gramine): A Review. *Pharm. Chem. J.* **2004**, *38*, 287–310.
- (61) Palmieri, A.; Petrini, M.; Shaikh, R. R. Synthesis of 3-substituted indoles via reactive alkylideneindolenine intermediates. *Org. Biomol. Chem.* **2010**, *8*, 1259–1270.
- (62) Ilic, N.; Habus, I.; Barkawi, L. S.; Park, S.; Stefanic, Z.; Kojic-Prodic, B.; Cohen, J. D.; Magnus, V. Aminoethyl-substituted indole-3-acetic acids for the preparation of tagged and carrier-linked auxin. *Bioorg. Med. Chem.* **2005**, *13*, 3229–3240.
- (63) Gonzalez-Lafuente, L.; Egea, J.; Leon, R.; Martinez-Sanz, F. J.; Monjas, L.; Perez, C.; Merino, C.; Garcia-De Diego, A. M.; Rodriguez-Franco, M. I.; Garcia, A. G.; Villarroja, M.; Lopez, M. G.; de Los Rios, C. Benzothiazepine CGP37157 and its isosteric 2'-methyl analogue provide neuroprotection and block cell calcium entry. *ACS Chem. Neurosci.* **2012**, *3*, 519–529.
- (64) Sousa, S. R.; Vetter, I.; Ragnarsson, L.; Lewis, R. J. Expression and pharmacology of endogenous Cav channels in SH-SY5Y human neuroblastoma cells. *PLoS One* **2013**, *8*, e59293.
- (65) Vaughan, P. F.; Peers, C.; Walker, J. H. The use of the human neuroblastoma SH-SY5Y to study the effect of second messengers on noradrenaline release. *Gen. Pharmacol.* **1995**, *26*, 1191–1201.
- (66) Reeve, H. L.; Vaughan, P. F.; Peers, C. Calcium channel currents in undifferentiated human neuroblastoma (SH-SY5Y) cells: actions and possible interactions of dihydropyridines and omega-conotoxin. *Eur. J. Neurosci.* **1994**, *6*, 943–952.

- (67) Albillos, A.; Garcia, A. G.; Olivera, B.; Gandia, L. Re-evaluation of the P/Q Ca²⁺ channel components of Ba²⁺ currents in bovine chromaffin cells superfused with solutions containing low and high Ba²⁺ concentrations. *Pflugers Arch.* **1996**, *432*, 1030–1038.
- (68) Arranz-Tagarro, J. A.; de los Rios, C.; Garcia, A. G.; Padin, J. F. Recent patents on calcium channel blockers: emphasis on CNS diseases. *Expert Opin. Ther. Pat.* **2014**, *24*, 959–977.
- (69) Hillyard, D. R.; Monje, V. D.; Mintz, I. M.; Bean, B. P.; Nadasdi, L.; Ramachandran, J.; Miljanich, G.; Azimi-Zoonooz, A.; McIntosh, J. M.; Cruz, L. J.; Imperial, J. S.; Olivera, B. M. A new Conus peptide ligand for mammalian presynaptic Ca²⁺ channels. *Neuron* **1992**, *9*, 69–77.
- (70) Xing, Y.; Xu, Y.; Chen, Y.; Jeffrey, P. D.; Chao, Y.; Lin, Z.; Li, Z.; Strack, S.; Stock, J. B.; Shi, Y. Structure of protein phosphatase 2A core enzyme bound to tumor-inducing toxins. *Cell* **2006**, *127*, 341–353.
- (71) Sun, L.; Liu, S. Y.; Zhou, X. W.; Wang, X. C.; Liu, R.; Wang, Q.; Wang, J. Z. Inhibition of protein phosphatase 2A- and protein phosphatase 1-induced tau hyperphosphorylation and impairment of spatial memory retention in rats. *Neuroscience* **2003**, *118*, 1175–1182.
- (72) Perez, M.; Hernandez, F.; Gomez-Ramos, A.; Smith, M.; Perry, G.; Avila, J. Formation of aberrant phosphotau fibrillar polymers in neural cultured cells. *Eur. J. Biochem.* **2002**, *269*, 1484–1489.
- (73) Swingle, M.; Ni, L.; Honkanen, R. E. Small-molecule inhibitors of ser/thr protein phosphatases: specificity, use and common forms of abuse. *Methods Mol. Biol.* **2007**, *365*, 23–38.
- (74) McAvoy, T.; Nairn, A. C. Serine/threonine protein phosphatase assays. *Curr. Protoc. Mol. Biol.* **2010**, *Chapter 18*, Unit18 18.

- (75) Denu, J. M.; Lohse, D. L.; Vijayalakshmi, J.; Saper, M. A.; Dixon, J. E. Visualization of intermediate and transition-state structures in protein-tyrosine phosphatase catalysis. *Proc. Natl. Acad. Sci. U S A* **1996**, *93*, 2493–2498.
- (76) Denizot, F.; Lang, R. Rapid colorimetric assay for cell growth and survival. Modifications to the tetrazolium dye procedure giving improved sensitivity and reliability. *J. Immunol. Methods* **1986**, *89*, 271–277.
- (77) Nicolau, S. M.; de Diego, A. M.; Cortes, L.; Egea, J.; Gonzalez, J. C.; Mosquera, M.; Lopez, M. G.; Hernandez-Guijo, J. M.; Garcia, A. G. Mitochondrial Na⁺/Ca²⁺-exchanger blocker CGP37157 protects against chromaffin cell death elicited by veratridine. *J. Pharmacol. Exp. Ther.* **2009**, *330*, 844–854.
- (78) Kolok, S.; Nagy, J.; Szombathelyi, Z.; Tarnawa, I. Functional characterization of sodium channel blockers by membrane potential measurements in cerebellar neurons: prediction of compound preference for the open/inactivated state. *Neurochem. Int.* **2006**, *49*, 593–604.
- (79) Koh, P. O. Melatonin attenuates decrease of protein phosphatase 2A subunit B in ischemic brain injury. *J. Pineal Res.* **2012**, *52*, 57–61.
- (80) Martinez-Sanz, F. J.; Lajarin-Cuesta, R.; Gonzalez-Lafuente, L.; Moreno-Ortega, A. J.; Punzon, E.; Cano-Abad, M. F.; de Los Rios, C. Neuroprotective profile of pyridothiazepines with blocking activity of the mitochondrial Na⁽⁺⁾/Ca⁽²⁺⁾ exchanger. *Eur. J. Med. Chem.* **2016**, *109*, 114–123.
- (81) Lewerenz, J.; Maher, P. Chronic Glutamate Toxicity in Neurodegenerative Diseases-What is the Evidence? *Front. Neurosci.* **2015**, *9*, 469.
- (82) Chan, S. F.; Sucher, N. J. An NMDA receptor signaling complex with protein phosphatase 2A. *J. Neurosci.* **2001**, *21*, 7985–7992.

- (83) Zimmer, E. R.; Leuzy, A.; Souza, D. O.; Portela, L. V. Inhibition of protein phosphatase 2A: focus on the glutamatergic system. *Mol. Neurobiol.* **2015**, DOI: 10.1007/s12035-015-9321-0
- (84) Triggle, D. J. Drug targets in the voltage-gated calcium channel family: why some are and some are not. *Assay Drug Dev. Technol.* **2003**, *1*, 719–733.
- (85) Baell, J. B.; Holloway, G. A. New substructure filters for removal of pan assay interference compounds (PAINS) from screening libraries and for their exclusion in bioassays. *J. Med. Chem.* **2010**, *53*, 2719–2740.
- (86) Na, Y. M.; Le Borgne, M.; Pagniez, F.; Le Baut, G.; Le Pape, P. Synthesis and antifungal activity of new 1-halogenobenzyl-3-imidazolylmethylindole derivatives. *Eur. J. Med. Chem.* **2003**, *38*, 75–87.
- (87) Evans, D. A.; Scheidt, K. A.; Fandrick, K. R.; Lam, H. W.; Wu, J. Enantioselective indole Friedel–Crafts alkylations catalyzed by bis(oxazolinyl)pyridine-scandium(III) triflate complexes. *J. Am. Chem. Soc.* **2003**, *125*, 10780–10781.
- (88) Evans, D. A.; Fandrick, K. R.; Song, H. J. Enantioselective Friedel–Crafts alkylations of α,β -unsaturated 2-acyl imidazoles catalyzed by bis(oxazolinyl)pyridine-scandium(III) triflate complexes. *J. Am. Chem. Soc.* **2005**, *127*, 8942–8943.
- (89) Haider, N.; Kabicher, T.; Kaferbock, J.; Plenk, A. Synthesis and in-vitro antitumor activity of 1-[3-(indol-1-yl)prop-1-yn-1-yl]phthalazines and related compounds. *Molecules* **2007**, *12*, 1900–1909.
- (90) Martelli, C.; Coronello, M.; Dei, S.; Manetti, D.; Orlandi, F.; Scapechi, S.; Novella Romanelli, M.; Salerno, M.; Mini, E.; Teodori, E. Structure-activity relationships studies in a series of N,N-bis(alkanol)amine aryl esters as P-glycoprotein (Pgp) dependent multidrug resistance (MDR) inhibitors. *J. Med. Chem.* **2010**, *53*, 1755–1762.

- (91) Henry, D. W.; Leete, E. Amine oxides. I. Gramine oxide. *J. Am. Chem. Soc.* **1957**, *79*, 5254–5256.
- (92) Miranda, S.; Lopez-Alvarado, P.; Avendano, C.; Menendez, J. C. Convenient synthesis of highly functionalized, 3,4-disubstituted indole building blocks. *Open Org. Chem. J.* **2007**, *1*, 1–12.
- (93) Thomsen, R.; Christensen, M. H. MolDock: a new technique for high-accuracy molecular docking. *J. Med. Chem.* **2006**, *49*, 3315–3321.
- (94) Moro, M. A.; Lopez, M. G.; Gandia, L.; Michelena, P.; Garcia, A. G. Separation and culture of living adrenaline- and noradrenaline-containing cells from bovine adrenal medullae. *Anal. Biochem.* **1990**, *185*, 243–248.
- (95) Hamill, O. P.; Marty, A.; Neher, E.; Sakmann, B.; Sigworth, F. J. Improved patch-clamp techniques for high-resolution current recording from cells and cell-free membrane patches. *Pflugers Arch.* **1981**, *391*, 85–100.

Table of Contents graphic

